https://ntrs.nasa.gov/search.jsp?R=19780022112 2020-03-22T03:45:30+00:00Z

NASA Technical Paper 1249

# Aerodynamic Characteristics at Mach 6 of a Wing-Body Concept for a Hypersonic Research Airplane

James L. Dillon and Jimmy L. Pittman

AUGUST 1978

NASA

NASA Technical Paper 1249

# Aerodynamic Characteristics at Mach 6 of a Wing-Body Concept for a Hypersonic Research Airplane

James L. Dillon and Jimmy L. Pittman
*Langley Research Center*
*Hampton, Virginia*

National Aeronautics
and Space Administration

**Scientific and Technical
Information Office**

1978

## SUMMARY

An experimental investigation of the static aerodynamic characteristics of a 1/30-scale model of a wing-body concept for a high-speed research airplane was conducted in the Langley 20-inch Mach 6 tunnel. The investigation consisted of configuration buildup from the basic body by adding a wing, center vertical tail, three-module scramjet, and six-module scramjet engine. The test Mach number was 6 at a Reynolds number, based on model fuselage length, of about $13.7 \times 10^6$. The test angle-of-attack range was $-4^\circ$ to $20^\circ$ at constant angles of sideslip of $0^\circ$, $-2^\circ$, and $-4^\circ$. The elevons were deflected from $10^\circ$ to $-15^\circ$ for pitch control. Roll and yaw control were investigated.

With a maximum of $-15^\circ$ of elevon deflection, the basic configuration was trimmable up to an angle of attack of approximately $21^\circ$ with a trimmed maximum lift-drag ratio $(L/D)_{max}$ of 3.1; addition of the scramjet engine reduced the maximum trim angle to $8.5^\circ$ and the maximum L/D attained to 2.6. Flaring the rudder or elevons was effective in controlling the longitudinal aerodynamic center. The concept was laterally unstable below an angle of attack of $3^\circ$ and directionally unstable across the test angle-of-attack range. Roll and yaw control were available through the test angle-of-attack range. The Hypersonic Arbitrary-Body Aerodynamic Computer Program gave good predictions for the longitudinal but not for the lateral-directional aerodynamic characteristics.


## INTRODUCTION

The National Aeronautics and Space Administration, The U.S. Air Force, and industry have studied numerous concepts relating to the development of hypersonic flight vehicles such as commercial transports, military vehicles, and airbreathing launch vehicles (e.g., ref. 1). The higher flight speeds will require the development of new systems such as propulsion, structures, airframe cooling, and cryogenic fuel storage. One industry study (ref. 2) concluded that both ground facilities and flight vehicles would be necessary to develop these advanced systems. Past experience with the "X" series of research aircraft (e.g., ref. 3) has shown that the air-launched, rocket-boosted, and glide-descent technique is an effective means of conducting flight research, and a number of studies of research aircraft concepts utilizing this technique have been conducted in recent years (e.g., refs. 4 and 5).

The purpose of the present investigation was to determine experimentally the hypersonic longitudinal, lateral, and directional stability and control characteristics of one

research airplane concept. This particular concept was a wing-body design that could be air launched from a B-52, rocket-boosted to about M = 6 (depending on mission objectives), and glide to an unpowered landing both with and without a scramjet engine attached. The tests include configuration buildup and elevon and rudder deflection. The investigation was conducted at Mach 6 and a Reynolds number of approximately $13.7 \times 10^6$ based on fuselage length. The angle-of-attack range was $-4^\circ$ to $20^\circ$ at constant angles of sideslip of $0^\circ$, $-2^\circ$, and $-4^\circ$. The elevons were deflected symmetrically to establish trim characteristics, asymmetrically for roll control, and split to form wedge elevons for longitudinal aerodynamic center control. The rudder was deflected for yaw control. Selected comparisons are made between data and predictions from the Hypersonic Arbitrary-Body Aerodynamics Computer Program (ref. 6). Most of the basic data and all the visual flow study results are presented in the appendixes. The results from tests at subsonic and transonic speeds on this same model are reported in references 7 and 8, respectively.

## SYMBOLS

The longitudinal characteristics are presented about the stability axis, and the lateral-directional characteristics about the body axis (fig. 1). The moment reference point was at the design center-of-gravity location which was 65 percent of the body length longitudinally and on the model reference line vertically (fig. 2). Values are given in SI Units. (Tables present values in both SI Units and U.S. Customary Units.) Measurements and calculations were made in U.S. Customary Units.

$A_b$ base area of fuselage, 0.0023 $m^2$

$A_r$ reference area, 0.0626 $m^2$

b wing span, 0.244 m

$C_D$ drag coefficient, $\frac{D}{q_\infty A_r}$

$C_{D,o}$ drag coefficient at zero lift

$C_L$ lift coefficient, $\frac{L}{q_\infty A_r}$

$C_l$ rolling-moment coefficient, $\frac{M_X}{q_\infty A_r b}$

$C_{l_\beta}$ effective dihedral parameter, $\frac{\Delta C_l}{\Delta \beta}$, per degree

$C_{l_{\delta_H}}$ rate of change of $C_l$ with differential elevon deflection, per degree, $\left(C_{l_{\delta_H=20}} - C_{l_{\delta_H=0}}\right) \Big/ 20$

$C_{l_{\delta_V}}$ rate of change of $C_l$ with rudder deflection, per degree

$C_m$ pitching-moment coefficient, $\frac{M_Y}{q_\infty A_r l}$

$C_{m,o}$ pitching-moment coefficient at zero lift

$\frac{\partial C_m}{\partial C_L}$ static longitudinal stability parameter, based on $l$

$C_n$ yawing-moment coefficient, $\frac{M_Z}{q_\infty A_r b}$

$C_{n_\beta}$ directional stability parameter, $\frac{\Delta C_n}{\Delta \beta}$, per degree

$C_{n_{\delta_H}}$ rate of change of $C_n$ with differential elevon deflection, per degree, $\left(C_{n_{\delta_H=20}} - C_{n_{\delta_H=0}}\right) \Big/ 20$

$C_{n_{\delta_V}}$ rate of change of $C_n$ with rudder deflection, per degree

$C_Y$ side-force coefficient, $\frac{F_Y}{q_\infty A_r}$

$C_{Y_\beta}$ side-force parameter, $\frac{\Delta C_Y}{\Delta \beta}$, per degree

$C_{Y_{\delta_H}}$ rate of change of $C_Y$ with differential elevon deflection, per degree, $\left(C_{Y_{\delta_H=20}} - C_{Y_{\delta_H=0}}\right) \Big/ 20$

$C_{Y_{\delta_V}}$ rate of change of $C_Y$ with rudder deflection, per degree

D drag, $F_N \sin \alpha + F_A \cos \alpha$

$F_A$ axial force along X-axis, positive direction, -X

$F_N$ normal force along Z-axis, positive direction, -Z

$F_Y$ side force along Y-axis, positive direction, +Y

L lift, $F_N \cos \alpha - F_A \sin \alpha$

$l$ length of model fuselage

L/D lift-drag ratio

$(L/D)_{max}$ maximum lift-drag ratio

M Mach number

$M_X, M_Y, M_Z$ moments about X-, Y-, and Z-axes, respectively

$q_\infty$ free-stream dynamic pressure

X,Y,Z reference axes, when unsubscripted they are body axes

x,y,z coordinates along X-, Y-, and Z-axes, respectively, cm

$\alpha$ angle of attack, deg

$\beta$ angle of sideslip, deg

$\Delta\beta$ $= (\beta \neq 0^{o}) - (\beta = 0^{o})$

$\delta_e$ elevon deflection angle, positive when trailing edge (T.E.) is down, deg

Subscripts:

s stability axis system

t trim condition, $C_m = 0$

$\delta_H$ differentially deflected ailerons for roll control, positive for T.E. down

$\delta_V$ deflected rudder for yaw control, positive for T.E. left

Abbreviations:

a.c. aerodynamic center

c.g. center of gravity, moment reference point

HL hinge line

L.E. leading edge

T.E. trailing edge

Model nomenclature:

B body or fuselage

BF base fairing

$BWV_{CH}$ basic configuration

| | |
|---|---|
| $BWV_{CH}E_6$ | complete configuration |
| $E_3$ | three-module scramjet engine |
| $E_6$ | six-module scramjet engine |
| $V_{CDB}$ | center vertical tail, speed brakes |
| $V_{CH}$ | center vertical tail, hypersonic (wedge airfoil) |
| $V_{CS}$ | center vertical tail, subsonic (diamond airfoil) |
| W | wing |

## DESIGN CONCEPT CONSIDERATIONS

The overall design rationale for this concept was primarily based on performance, stability, and control requirements at Mach numbers from 6 to 8 and the performance at touchdown speed, with the scramjet engine installed. It has been shown in reference 9 that vehicle performance is sensitive to the scramjet engine longitudinal location and to wing incidence since the airframe-integrated scramjet concept uses the forebody for precompressed air and the aftbody for a half nozzle expansion ramp (ref. 10). A three-module scramjet engine package is considered the minimum number of engines to make a meaningful flight experiment whereas a six-module package is representative of the size required to produce positive net thrust at Mach 6. The center vertical tail was designed with a dual hinge line rudder at approximately the two-thirds chord location to allow for a diamond airfoil for subsonic through supersonic speeds, a wedge airfoil for hypersonic speeds, and for speed brake extension. The elevons were envisioned to be split in order to provide flared elevons for longitudinal aerodynamic center control.

The Hypersonic Arbitrary-Body Aerodynamics Computer Program (ref. 6) with simplified geometry input from reference 11 was used for hypersonic aerodynamic predictions during parametric studies to define this concept. Several available options within this program have been exercised to compare with hypersonic aerodynamics data (e.g., refs. 12, 13, and 14). For the research airplane concept analyzed in this paper, the following options were utilized for theoretical predictions: for compression regions, tangent cone on the fuselage and tangent wedge on the wing and vertical tail; for expansion regions, Prandtl-Meyer expansion; and for skin friction, the Spalding-Chi method (with 100-percent turbulent boundary layer). The numerical model that was used for the aerodynamic predictions is presented in table I.

## APPARATUS AND METHODS

### Model

A sketch and a photograph of the model with its interchangeable parts are shown in figures 2 and 3, respectively. The 1/30-scale test model was of modular design to permit buildup of the basic model (fig. 2(a)) from components consisting of body, cropped delta wing, center vertical tail, and scramjet engine. The wing had $2.1^{\circ}$ negative incidence and $10^{\circ}$ dihedral. The airfoil was a modified circular arc with a leading-edge radius (normal to L.E.) of 0.064 cm followed by a $10^{\circ}$ wedge section. The elevons had a constant thickness at the hinge line of 0.814 cm and $7.6^{\circ}$ wedge angle and were contoured on top and bottom over approximately the aft one-third to give a trailing-edge thickness of 0.064 cm. Two model scramjet engine packages consisting of three and six clustered modules were also tested. (See figs. 2(b) and 3.) The actual scramjet engine would have three internal fuel struts in each module whereas the model engine packages used in this test simulated the internal geometric contraction by use of one strut. The dual hinge-line rudder variations were simulated with three separate vertical tails (figs. 2(c) and 3). The flared elevons were simulated by deflecting the elevons $-5^{\circ}$ and attaching $10^{\circ}$ wedges on the flat lower surface. The pertinent geometrical characteristics of the model for aerodynamic testing are listed in table II.

### Wind Tunnel and Test Conditions

The investigation was conducted in the Langley 20-inch Mach 6 tunnel. This is a blowdown type wind tunnel which exhausts into the atmosphere or vacuum spheres. The tunnel has a two-dimensional nozzle and a test section 52.1 cm high and 50.8 cm wide. More detailed description of this tunnel can be found in reference 15.

The tests were conducted at Mach 6 and at a nominal stagnation pressure and temperature of 3034 $kN/m^2$ and 500 K, respectively. The corresponding free-stream Reynolds number per meter was $23.5 \times 10^6$. Aerodynamic force and moment data were obtained over an angle-of-attack range of $-4^{\circ}$ to $20^{\circ}$ and for angles of sideslip of $0^{\circ}$, $-2^{\circ}$, and $-4^{\circ}$. Elevon deflections were varied from $10^{\circ}$ to $-15^{\circ}$ and the rudder was deflected $0^{\circ}$ and $-15.4^{\circ}$.

### Data Acquisition and Reduction

Aerodynamic force and moment data were measured with a six-component strain-gage balance which was housed inside the model fuselage and attached to the tunnel sting support system. The movable sting support system was pneumatically driven through the angle-of-attack range during each run. Angles of sideslip were obtained by rotating the

support system to the desired offset angle prior to an excursion through the angle-of-attack range. The angles of attack and sideslip were set optically by using a prism mounted on the model to reflect a point source of light onto a calibrated chart. The Mach number was obtained with a total-pressure probe which was inserted into the test section upstream of the model at the beginning and end of each run. (Force data were not recorded with the probe in the tunnel.) The Mach number for each test point was then determined by linear interpolation with time.

Straight-line slopes between the data at $\beta = 0^{\circ}$ and $\beta = -2^{\circ}$ or $-4^{\circ}$ were used to obtain the lateral-directional stability parameters. Model base pressure was determined from the average measurements made at three locations with forward-facing pressure tubes during each test (fig. 2(a)), and the axial-force data were adjusted to correspond to a base pressure equal to free-stream static pressure.

Schlieren and oil-flow photographs were also obtained during the test program. The oil-flow study was conducted separately from the force study.

## RESULTS AND DISCUSSION

### Static Longitudinal Characteristics

Configuration buildup and effect of components.- The longitudinal aerodynamic characteristics for the configuration buildup are presented in figure 4. Addition of the wing to the body stabilized this combination through the test angle-of-attack range. Addition of the wedge tail and either the three- or six-module scramjet engine was a stabilizing influence but each component produced succeedingly lower lift-drag ratios. Note that $C_{m,o}$ for the complete configuration $\left(BWV_{CH}E_6\right)$ is about the same as that for the body-wing (BW); that is, the increase in $C_{m,o}$ from addition of the vertical tail is offset by a decrease when the six-module scramjet is installed.

The effect of vertical-tail variations on the basic and complete configurations is presented in figures 5 and 6. Closing the split rudder to form a diamond airfoil vertical tail produced a slight increase in $L/D$ but negligible change in the aerodynamic center. Conversely, flaring the split rudder to form speed brakes was effective in producing an increment in $C_{m,o} = 0.022$ relative to the hypersonic wedge tail, a slight rearward shift in aerodynamic center, and an increment in $C_{D,o} = 0.006$, the effect on drag decreasing with increasing angle of attack.

Trim characteristics.- The effect of elevon deflection on the longitudinal characteristics of the configurations with and without the six-module scramjet engine is presented in appendix A. These effects were used to determine the trimmed characteristics for the basic and complete configurations which are presented in figures 7 and 8, respectively.

With a maximum of $-15^{\circ}$ of elevon deflection, the basic configuration was trimmable up to an angle of attack of about $21^{\circ}$ and had a trimmed $(L/D)_{max}$ of 3.1; addition of the scramjet engine reduced the maximum trim angle of attack to $8.5^{\circ}$ and the maximum L/D attained was 2.6. The low values of maximum trim angle of attack for the complete configuration resulted from the low positive value of $C_{m,o}$ and low elevon deflection effectiveness. (See appendix A.) However, the trim angle-of-attack range resulting from this investigation is adequate for the low cruise angle of attack envisioned for this airplane (ref. 8). The trimmed static margin for the basic and complete configurations varied from 2 percent to 6 percent of the model fuselage length over the trimmed angle-of-attack range.

Wedge elevons.- The results of the wedge-elevon investigation are presented in figure 9. These deflections result in an untrimmed static margin gain of 1.7 percent and 1.4 percent for the basic and complete configurations, respectively, relative to the zero elevon deflection case. The effectiveness of wedge airfoil surfaces for enhancing directional stability was proven during the X-15 research program (ref. 16). It appears that this same approach may be used to minimize longitudinal aerodynamic center shift and reduce trim losses across the Mach number range but more investigation is needed.

## Static Lateral-Directional Characteristics

Configuration buildup.- The static lateral-directional characteristics for the body buildup were evaluated for $\Delta\beta = -2^{\circ}$ and $\Delta\beta = -4^{\circ}$. The characteristics for $\Delta\beta = -2^{\circ}$ are presented in figure 10 and those for $\Delta\beta = -4^{\circ}$ in appendix B. The body alone is unstable both laterally and directionally across the test angle-of-attack range. Addition of the wing produces lateral stability above about $9^{\circ}$ but this configuration remains directionally unstable. Addition of the vertical tail and either of the scramjet engine packages was a stabilizing influence but these components provided lateral stability only for $\alpha > 3^{\circ}$ and the configurations remain either neutral or unstable directionally across the test angle-of-attack range. Therefore, modifications appear necessary for this concept to be acceptable from a static stability viewpoint at $M = 6$.

Roll and yaw control.- The roll control characteristics for the basic and complete configurations are presented in figure 11. These data were obtained by deflecting the left elevon $10^{\circ}$ and the right elevon $-10^{\circ}$. Roll control is available for both the basic and complete configurations. The yawing moment due to roll control is adverse and increases with increasing angle of attack. Note that the effects of adding the engine are negligible on $C_{l_{\delta_H}}$ and $C_{Y_{\delta_H}}$.

The yaw characteristics for the basic and complete configurations are presented in figure 12. These data were obtained by deflecting the rudder $-15.4^{\circ}$. The rolling moment

due to yaw control $C_{l_{\delta_V}}$ for both configurations is about equal to the roll control effectiveness $C_{l_{\delta_H}}$ for $\alpha \lesssim 5^{\circ}$; at higher angles of attack, $C_{l_{\delta_V}}$ decreases with increasing $\alpha$. Rudder effectiveness is available through the test angle-of-attack range but it decreases with increasing angle of attack. Again, addition of the engine had a negligible effect on the yaw control.

## Theoretical Comparison

Longitudinal body buildup.- The theoretical predictions from the method of reference 6 for the longitudinal aerodynamic characteristics for the B, BW, and $BWV_{CH}$ configurations are compared with the experimental data in figure 13. The predictions are seen to be good but, in general, at the lower angles of attack the lift is underpredicted and drag and pitching moment overpredicted whereas at the higher angles of attack the lift is overpredicted and the drag and pitching moment are underpredicted.

Trim characteristics.- The theoretical trimmed aerodynamic characteristics for the basic configuration are compared with experimental data in figure 14. These theoretical results were obtained from the predicted aerodynamic characteristics for various elevon deflections as shown in appendix A. The predicted trimmed lift-drag ratio is seen to be higher than the data for $C_L > 0.14$ but $(L/D)_{max}$ is almost identical to the data. The trimmed static margin is overpredicted by about 1 percent at the higher $C_L$ levels.

Lateral-directional stability.- The theoretical lateral-directional stability parameters are compared with experimental data in figure 15. The predicted lateral stability characteristics for the body alone agree with the data in trend and magnitude whereas the stable region attained by addition of the wing is predicted but the magnitude is incorrect. The $BWV_{CH}$ configuration is predicted to be laterally stable across the test angle-of-attack range but the data show it to be unstable for $\alpha < 4^{\circ}$. The experimental directional stability level and trend is well predicted for B and BW configurations; however, the overall trend and magnitude are in error when the tail is added to form $BWV_{CH}$. In summary, the theory tends to predict the stability parameters rather well for the isolated body but not for combinations of components. These results are probably due to the inability of the theory to accurately predict the pressure distribution or to account for component interference.

## CONCLUSIONS

An investigation has been conducted to determine the hypersonic aerodynamic characteristics of a wing-body concept for a hypersonic research airplane. The investigation

was conducted at a Mach number of 6 and at a Reynolds number per meter of $23.5 \times 10^6$. An analysis of the data leads to the following conclusions:

1. With a maximum elevon deflection of $-15^\circ$, the basic configuration was trimmable to an angle of attack of $21^\circ$ and had a trimmed maximum lift-drag ratio $(L/D)_{max}$ of 3.1; addition of a six-module scramjet reduced the maximum trimmed angle of attack to $8.5^\circ$ and the $(L/D)_{max}$ attained was 2.6.

2. Flaring the split rudder to form speed brakes improved longitudinal stability.

3. Wedge elevons were effective in shifting the aerodynamic center rearward by 1.7 percent and 1.4 percent of fuselage length for the basic and complete configurations, respectively.

4. This concept was unstable laterally for an angle of attack less than $3^\circ$ and either neutral or unstable directionally across the test angle-of-attack range.

5. Roll and yaw control were available through the test angle-of-attack range. Yaw due to roll control became sizable at the higher angles of attack whereas the roll due to yaw control was equal to roll control effectiveness at low angles of attack.

6. The Hypersonic Arbitrary-Body Aerodynamics Computer Program gave reasonable predictions of longitudinal aerodynamic characteristics; however, lateral-directional stability parameters were not well predicted except for the isolated body.

Langley Research Center
National Aeronautics and Space Administration
Hampton, VA 23665
May 16, 1978

## APPENDIX A

## EFFECT OF ELEVON DEFLECTION

The effects of elevon deflection on the longitudinal characteristics of the basic and complete configurations are presented in figures 16 and 17, respectively. Theoretical predictions from the methods of references 6 and 11 compared with experimental data for the basic configuration are shown in figure 18. These data and predictions were used to determine the trimmed longitudinal characteristics for this concept with and without the scramjet engine installed. Note that the effect of negative elevon deflection is small and that the complete configuration has a very small positive $C_{m,o}$.

The theory is noted to underpredict the lift at the lower angles of attack and overpredict lift at the higher angles of attack. The $C_{D,o}$ predictions are good in general but $C_{m,o}$ is overpredicted as is the effect of elevon deflection on the pitching moment $\partial C_m/\partial \delta_e$. The predicted level of $(L/D)_{max}$ is good but the angle of attack at which it occurs does not correspond to the data. Likewise, the static margin at trim is predicted very well but the angle of attack for $C_{m,o}$ is not.

## APPENDIX B

## LATERAL-DIRECTIONAL STABILITY DERIVATIVES

The static lateral-directional stability characteristics for body buildup evaluated at $\Delta\beta = -4^{\circ}$ is presented in figure 19. These data were compared with those for $\Delta\beta = -2^{\circ}$ (fig. 10) and are seen to be almost identical. Therefore, the basic lateral-directional characteristics are assumed to be linear over the range $-4^{\circ} \leq \beta \leq 4^{\circ}$ for the test angle-of-attack range. Those stability characteristics for $\Delta\beta = -2^{\circ}$ are shown in the text of this paper since they are considered to be more accurate than results obtained at $\Delta\beta = -4^{\circ}$ because of less balance interactions.

## APPENDIX C

## VISUAL FLOW PHOTOGRAPHS

Visual observations that were recorded as a part of this test program are included for quantitative assessment of this design concept.

A schlieren photograph of the model at an angle of attack of $20^{\circ}$ is shown in figure 20. Shocks from the nose, canopy, wing, and tail are readily identified as is the expansion region aft of the canopy. The complexity of the flow in the vicinity of the engine is also demonstrated by the multitude of interacting shocks.

Oil-flow patterns at various model attitudes are presented in figure 21. The model is shown at zero sideslip angle and angles of attack of $0^{\circ}$, $4^{\circ}$, and $8^{\circ}$ in figure 21(a). Observations in the top view (A, D, and H) are the forward movement of the shear line on the wings with increasing angle of attack, apparent separation in front of the canopy windscreen, and disturbances from the canopy itself which form counterrotating vortices along the top of the fuselage. Views B, E, and J again show disturbances from the cockpit and the upward flow along the fuselage with separation and reattachment lines for the vortex. Note also the distinct shear line on the engine sidewall at $\alpha = 0^{\circ}$ and $4^{\circ}$ (B and E) which disappears at $\alpha = 8^{\circ}$ (J); this suggests inlet spillage which is influenced by angle of attack. The bottom views (C, F, G, and H) also show interesting flow patterns: inward flow on the wing at $\alpha = 0^{\circ}$ (leeside flow for this attitude) which straightens as angle of attack is increased; little shear flow behind the engine at $\alpha = 0^{\circ}$ but stronger shear with increasing $\alpha$ (this could be associated with the shear line noted on the engine sidewall); no disturbance on the wing due to the engine installation (F and G); and cross-flow on the forebody with separation or low shear areas which decrease with increasing $\alpha$. The flow patterns on the undersurface of the forebody forward of the break in the projected body sweep angle are similar to those found in reference 17 during heat-transfer tests on a hypersonic research airplane concept. The tests in reference 17 were conducted at $\alpha = 4^{\circ}$ and showed a separation region aft of the nose and a "cold streak" on the fuselage center line which persisted to the engine inlet location. The "cold streak" was assumed to result from a thickened boundary layer and inward cross flow. The model in reference 17 had a constant projected fuselage sweep angle from the nose to the engine inlet whereas the model in this test had a "break" approximately 60 percent of the distance from the nose to the engine inlet; therefore, the flow on the model in this test appears to be straighter well forward of the inlet station, possibly because of pressure relief at the fuselage break.

Since this airplane is envisioned to fly a research cruise segment at $\alpha = 4^{\circ}$, oil-flow patterns were also recorded at $\alpha = 4^{\circ}$ and $\beta = -4^{\circ}$ (fig. 21(b)). The strong

disturbances are again noted around the cockpit as well as separation and reattachment lines from vortices on top of the fuselage aft of the cockpit. The reattachment lines are shifted expectedly to the leeward side of the fuselage and appear to be much stronger on the leeward side than on the windward wide of the vertical tail (views A, G, and H). This flow pattern may help explain the directional instability noted from the force data analysis. The disturbance on the engine sidewall is again noted (views C and G) for this model attitude. The flow direction in yaw on the lower forebody is nearly identical to the vehicle yaw angle (view E) and may become a major design consideration in integrating fixed geometry scramjets which utilize sidewall internal compression such as the Langley concept employed in these tests. The degree of sidewise flow angularity which can be tolerated at the inlet of this concept has not been resolved.

## REFERENCES


1. Hearth, Donald P.; and Preyss, Albert E.: Hypersonic Technology – Approach to an Expanded Program. Astronaut. & Aeronaut., vol. 14, no. 12, Dec. 1976, pp. 20-37.

2. Hypersonic Research Facilities Study. Volume IV, Part 1, Phase III Final Studies – Flight Research Facilities. NASA CR-114327, 1970.

3. Eppley, C. V.: The Rocket Research Aircraft Program 1946-1962. FTC-TDR-63-3, U.S. Air Force, Feb. 1963.

4. Penland, Jim A.; Fournier, Roger H.; and Marcum, Don C., Jr.: Aerodynamic Characteristics of a Hypersonic Research Airplane Concept Having a $70^{\circ}$ Swept Double-Delta Wing at Mach Numbers From 1.50 to 2.86. NASA TN D-8065, 1975.

5. Kirkham, F. S.; Jackson, L. Robert; and Weidner, John P.: Study of a High-Speed Research Airplane. J. Aircr., vol. 12, no. 11, Nov. 1975, pp. 857-863.

6. Gentry, Arvel E.; and Smyth, Douglas N.: Hypersonic Arbitrary-Body Aerodynamic Computer Program (Mark III Version). Vol. II – Program Formulation and Listings. Rep. DAC 61552, Vol. II (Air Force Contract Nos. F33615 67 C 1008 and F33615 67 C 1602), McDonnell Douglas Corp., Apr. 1968. (Available from DDC as AD 851 812.)

7. Dillon, James L.; and Creel, Theodore R., Jr.: Aerodynamic Characteristics at Mach Number 0.2 of a Wing-Body Concept for a Hypersonic Research Airplane. NASA TP-1189, 1978.

8. Dillon, James L.; and Pittman, Jimmy L.: Aerodynamic Characteristics at Mach Numbers From 0.33 to 1.20 of a Wing-Body Design Concept for a Hypersonic Research Airplane. NASA TP-1044, 1977.

9. Weidner, J. P.; Small, W. J.; and Penland, J. A.: Scramjet Integration on Hypersonic Research Airplane Concepts. J. Aircr., vol. 14, no. 5, May 1977, pp. 460-466.

10. Henry, John R.; and Anderson, Griffin Y.: Design Considerations for the Airframe-Integrated Scramjet. NASA TM X-2895, 1973.

11. Stack, Sharon H.; Edwards, Clyde L. W.; and Small, William J.: GEMPAK: An Arbitrary Aircraft Geometry Generator. NASA TP-1022, 1977.

12. Ellison, James C.: Investigation of the Aerodynamic Characteristics of a Hypersonic Transport Model at Mach Numbers to 6. NASA TN D-6191, 1971.

13. Goldberg, Theodore J.; Hefner, Jerry N.; and Stone, David R.: Hypersonic Aerodynamic Characteristics of Two Delta-Wing X-15 Airplane Configurations. NASA TN D-5498, 1969.

14. Clark, Louis E.; and Richie, Christine B.: Aerodynamic Characteristics at Mach 6 of a Hypersonic Research Airplane Concept Having a $70^{\circ}$ Swept Delta Wing. NASA TM X-3475, 1977.

15. Keyes, J. Wayne: Force Testing Manual for the Langley 20-Inch Mach 6 Tunnel. NASA TM-74026, 1977.

16. McLellan, Charles H.: A Method for Increasing the Effectiveness of Stabilizing Surfaces at High Supersonic Mach Numbers. NACA RM L54F21, 1954.

17. Lawing, Pierce L.; and Hunt, James L.: Aerodynamic Heat Transfer to a Hypersonic Research Aircraft Model (X-24C) at Mach 6. J. Aircr., vol. 13, no. 12, Dec. 1976, pp. 1018-1020.

TABLE I.- THEORETICAL MODEL COORDINATES

(a) Fuselage coordinates

| x/l | y | | z | |
|---|---|---|---|---|
| | cm | in. | cm | in. |
| 0 | 0.000 | 0.000 | -0.737 | -0.290 |
| 0.002 | 0.000 | 0.000 | -0.576 | -0.227 |
| | .049 | .019 | -.583 | -.230 |
| | .094 | .037 | -.606 | -.238 |
| | .130 | .051 | -.641 | -.252 |
| | .153 | .060 | -.685 | -.270 |
| | .161 | .063 | -.734 | -.289 |
| | .153 | .060 | -.781 | -.307 |
| | .128 | .050 | -.820 | -.323 |
| | .091 | .036 | -.849 | -.334 |
| | .047 | .018 | -.866 | -.341 |
| | .000 | .000 | -.872 | -.343 |
| 0.045 | 0.000 | 0.000 | -0.077 | -0.030 |
| | .175 | .069 | -.111 | -.044 |
| | .326 | .128 | -.205 | -.081 |
| | .439 | .173 | -.343 | -.135 |
| | .508 | .200 | -.507 | -.200 |
| | .531 | .209 | -.684 | -.269 |
| | .529 | .208 | -.869 | -.342 |
| | .464 | .183 | -1.043 | -.411 |
| | .344 | .135 | -1.185 | -.466 |
| | .183 | .072 | -1.277 | -.503 |
| | .001 | .000 | -1.309 | -.516 |
| 0.132 | 0.000 | 0.000 | 0.930 | 0.366 |
| | .425 | .167 | .840 | .331 |
| | .787 | .310 | .598 | .236 |
| | 1.059 | .417 | .258 | .102 |
| | 1.236 | .487 | -.141 | -.055 |
| | 1.319 | .519 | -.569 | -.224 |
| | 1.319 | .519 | -.611 | -.240 |
| | 1.327 | .522 | -.951 | -.374 |
| | 1.284 | .506 | -1.289 | -.507 |
| | 1.178 | .464 | -1.612 | -.635 |
| | .983 | .387 | -1.889 | -.744 |
| | .675 | .266 | -2.019 | -.795 |
| | .000 | .000 | -2.019 | -.795 |
| 0.182 | 0.000 | 0.000 | 1.508 | 0.594 |
| | .527 | .208 | 1.413 | .556 |
| | .991 | .390 | 1.145 | .451 |
| | 1.351 | .532 | .747 | .294 |
| | 1.586 | .624 | .265 | .104 |
| | 1.687 | .664 | -.262 | -.103 |
| | 1.713 | .674 | -.262 | -.103 |
| | 1.765 | .695 | -1.227 | -.483 |
| | 1.691 | .666 | -1.479 | -.582 |
| | 1.598 | .629 | -1.725 | -.679 |
| | 1.482 | .584 | -1.960 | -.772 |
| | 1.332 | .525 | -2.176 | -.857 |
| | 1.113 | .438 | -2.310 | -.909 |
| | .000 | .000 | -2.310 | -.909 |
| 0.212 | 0.000 | 0.000 | 2.460 | 0.969 |
| | .022 | .009 | 2.454 | .966 |
| | .040 | .016 | 2.440 | .960 |
| | .067 | .026 | 2.403 | .946 |
| | .077 | .030 | 2.383 | .938 |
| | .587 | .231 | 1.594 | .628 |
| | .999 | .393 | 1.376 | .542 |
| | 1.355 | .533 | 1.074 | .423 |
| | 1.634 | .643 | .700 | .276 |
| | 1.823 | .718 | .273 | .108 |
| | 1.908 | .751 | -.185 | -.073 |
| | 1.949 | .767 | -.185 | -.073 |
| | 2.032 | .800 | -1.486 | -.585 |
| | 1.965 | .774 | -1.723 | -.678 |
| | 1.874 | .738 | -1.951 | -.768 |
| | 1.754 | .691 | -2.166 | -.853 |
| | 1.596 | .628 | -2.353 | -.926 |
| | 1.376 | .542 | -2.453 | -.966 |
| | .000 | .000 | -2.453 | -.966 |

TABLE I.- Continued

(a) Continued

| x/l | y | | z | |
|---|---|---|---|---|
| | cm | in. | cm | in. |
| 0.254 | 0.000 | 0.000 | 3.110 | 1.224 |
| | .130 | .051 | 3.098 | 1.220 |
| | .254 | .100 | 3.059 | 1.204 |
| | .368 | .145 | 2.996 | 1.180 |
| | .470 | .185 | 2.914 | 1.147 |
| | .555 | .218 | 2.815 | 1.108 |
| | 1.225 | .482 | 1.822 | .717 |
| | 1.547 | .609 | 1.495 | .589 |
| | 1.817 | .716 | 1.124 | .443 |
| | 2.030 | .799 | .718 | .283 |
| | 2.177 | .857 | .283 | .111 |
| | 2.250 | .886 | -.170 | -.067 |
| | 2.280 | .897 | -.170 | -.067 |
| | 2.407 | .948 | -1.769 | -.696 |
| | 2.351 | .926 | -1.993 | -.785 |
| | 2.262 | .890 | -2.205 | -.868 |
| | 2.135 | .840 | -2.398 | -.944 |
| | 1.962 | .773 | -2.551 | -1.004 |
| | 1.744 | .686 | -2.618 | -1.031 |
| | .000 | .000 | -2.618 | -1.031 |
| 0.297 | 0.000 | 0.000 | 3.275 | 1.289 |
| | .344 | .136 | 3.190 | 1.256 |
| | .662 | .261 | 3.031 | 1.193 |
| | .953 | .375 | 2.828 | 1.114 |
| | 1.221 | .481 | 2.594 | 1.021 |
| | 1.464 | .576 | 2.335 | .919 |
| | 1.718 | .676 | 1.881 | .740 |
| | 1.978 | .779 | 1.497 | .589 |
| | 2.203 | .867 | 1.092 | .430 |
| | 2.388 | .940 | .668 | .263 |
| | 2.525 | .994 | .226 | .089 |
| | 2.601 | 1.024 | -.231 | -.091 |
| | 2.790 | 1.099 | -1.981 | -.780 |
| | 2.749 | 1.082 | -2.204 | -.868 |
| | 2.661 | 1.047 | -2.413 | -.950 |
| | 2.524 | .994 | -2.594 | -1.021 |
| | 2.340 | .921 | -2.725 | -1.073 |
| | 2.120 | .835 | -2.775 | -1.093 |
| | .000 | .000 | -2.775 | -1.093 |

| x/l | y | | z | |
|---|---|---|---|---|
| | cm | in. | cm | in. |
| 0.408 | 0.000 | 0.000 | 3.377 | 1.330 |
| | .560 | .220 | 3.306 | 1.301 |
| | 1.090 | .429 | 3.111 | 1.225 |
| | 1.574 | .620 | 2.820 | 1.110 |
| | 2.004 | .789 | 2.454 | .966 |
| | 2.373 | .934 | 2.026 | .798 |
| | 3.382 | 1.332 | .702 | .276 |
| | 3.502 | 1.379 | .465 | .183 |
| | 3.578 | 1.408 | .211 | .083 |
| | 3.628 | 1.428 | -.050 | -.020 |
| | 3.658 | 1.440 | -.314 | -.124 |
| | 3.672 | 1.446 | -.579 | -.228 |
| | 3.780 | 1.488 | -2.430 | -.957 |
| | 3.756 | 1.479 | -2.654 | -1.045 |
| | 3.667 | 1.444 | -2.860 | -1.126 |
| | 3.520 | 1.386 | -3.030 | -1.193 |
| | 3.326 | 1.310 | -3.143 | -1.237 |
| | 3.105 | 1.223 | -3.183 | -1.253 |
| | .000 | .000 | -3.183 | -1.253 |
| 0.531 | 0.000 | 0.000 | 3.138 | 1.235 |
| | .674 | .265 | 3.082 | 1.213 |
| | 1.330 | .523 | 2.914 | 1.147 |
| | 1.946 | .766 | 2.636 | 1.038 |
| | 2.499 | .984 | 2.247 | .885 |
| | 2.962 | 1.166 | 1.754 | .691 |
| | 4.169 | 1.641 | .201 | .079 |
| | 4.292 | 1.690 | -.038 | -.015 |
| | 4.392 | 1.729 | -.288 | -.113 |
| | 4.466 | 1.758 | -.546 | -.215 |
| | 4.508 | 1.775 | -.812 | -.320 |
| | 4.514 | 1.777 | -1.081 | -.426 |
| | 4.692 | 1.847 | -2.928 | -1.153 |
| | 4.630 | 1.823 | -3.146 | -1.238 |
| | 4.514 | 1.777 | -3.340 | -1.315 |
| | 4.350 | 1.713 | -3.496 | -1.376 |
| | 4.148 | 1.633 | -3.598 | -1.417 |
| | 3.925 | 1.545 | -3.634 | -1.431 |
| | .000 | .000 | -3.634 | -1.431 |

TABLE I.- Continued

(a) Concluded

| x/l | y | | z | |
|---|---|---|---|---|
| | cm | in. | cm | in. |
| 0.561 | 0.000 | 0.000 | 3.079 | 1.212 |
| | .672 | .264 | 3.023 | 1.190 |
| | 1.324 | .521 | 2.853 | 1.123 |
| | 1.936 | .762 | 2.572 | 1.013 |
| | 2.485 | .978 | 2.181 | .859 |
| | 2.944 | 1.159 | 1.688 | .665 |
| | 4.201 | 1.654 | .079 | .031 |
| | 4.333 | 1.706 | -.158 | -.062 |
| | 4.447 | 1.751 | -.403 | -.159 |
| | 4.540 | 1.788 | -.657 | -.259 |
| | 4.606 | 1.813 | -.920 | -.362 |
| | 4.625 | 1.821 | -1.189 | -.468 |
| | 4.802 | 1.891 | -3.049 | -1.201 |
| | 4.746 | 1.869 | -3.265 | -1.285 |
| | 4.634 | 1.824 | -3.456 | -1.361 |
| | 4.473 | 1.761 | -3.610 | -1.421 |
| | 4.275 | 1.683 | -3.709 | -1.460 |
| | 4.055 | 1.597 | -3.744 | -1.474 |
| | .000 | .000 | -3.744 | -1.474 |
| 0.751 | 0.000 | 0.000 | 2.710 | 1.067 |
| | .656 | .258 | 2.649 | 1.043 |
| | 1.290 | .508 | 2.468 | .972 |
| | 1.879 | .740 | 2.171 | .855 |
| | 2.400 | .945 | 1.767 | .696 |
| | 2.832 | 1.115 | 1.269 | .500 |
| | 4.389 | 1.728 | -.696 | -.274 |
| | 4.398 | 1.731 | -.738 | -.291 |
| | 4.408 | 1.735 | -.781 | -.307 |
| | 4.418 | 1.739 | -.823 | -.324 |
| | 4.430 | 1.744 | -.865 | -.341 |
| | 4.716 | 1.857 | -.869 | -.342 |
| | 4.899 | 1.929 | -3.819 | -1.503 |
| | 4.878 | 1.920 | -4.010 | -1.579 |
| | 4.794 | 1.887 | -4.184 | -1.647 |
| | 4.659 | 1.834 | -4.323 | -1.702 |
| | 4.488 | 1.767 | -4.411 | -1.737 |
| | 4.297 | 1.692 | -4.441 | -1.749 |
| | .000 | .000 | -4.441 | -1.749 |

| x/l | y | | z | |
|---|---|---|---|---|
| | cm | in. | cm | in. |
| 0.830 | 0.000 | 0.000 | 2.844 | 1.120 |
| | .681 | .268 | 2.730 | 1.075 |
| | 1.310 | .516 | 2.442 | .961 |
| | 1.872 | .737 | 2.038 | .802 |
| | 2.365 | .931 | 1.551 | .611 |
| | 2.785 | 1.096 | 1.001 | .394 |
| | 4.117 | 1.621 | -.675 | -.266 |
| | 4.656 | 1.833 | -.675 | -.266 |
| | 4.903 | 1.930 | -4.138 | -1.629 |
| | 4.889 | 1.925 | -4.313 | -1.698 |
| | 4.825 | 1.899 | -4.475 | -1.762 |
| | 4.713 | 1.855 | -4.610 | -1.815 |
| | 4.563 | 1.796 | -4.700 | -1.850 |
| | 4.391 | 1.729 | -4.731 | -1.863 |
| | .000 | .000 | -4.731 | -1.863 |
| 0.870 | 0.000 | 0.000 | 2.912 | 1.146 |
| | .700 | .276 | 2.776 | 1.093 |
| | 1.333 | .525 | 2.445 | .963 |
| | 1.887 | .743 | 1.993 | .785 |
| | 2.363 | .930 | 1.459 | .575 |
| | 2.761 | 1.087 | .865 | .341 |
| | 3.839 | 1.512 | -.671 | -.264 |
| | 4.574 | 1.801 | -.671 | -.264 |
| | 4.905 | 1.931 | -3.585 | -1.411 |
| | 4.897 | 1.928 | -3.719 | -1.464 |
| | 4.848 | 1.909 | -3.844 | -1.514 |
| | 4.761 | 1.875 | -3.947 | -1.554 |
| | 4.646 | 1.829 | -4.016 | -1.581 |
| | 4.513 | 1.777 | -4.039 | -1.590 |
| | .000 | .000 | -4.039 | -1.590 |
| 1.000 | 0.000 | 0.000 | 3.133 | 1.233 |
| | .744 | .293 | 2.821 | 1.111 |
| | 1.432 | .564 | 2.400 | .945 |
| | 2.033 | .801 | 1.864 | .734 |
| | 2.491 | .981 | 1.201 | .473 |
| | 2.684 | 1.057 | .423 | .167 |
| | 2.684 | 1.057 | -.923 | -.363 |
| | 4.911 | 1.933 | -.923 | -.363 |
| | 4.911 | 1.933 | -1.761 | -.693 |
| | .000 | .000 | -1.761 | -.693 |

TABLE I.- Continued

(b) Wing coordinates

| Chord | Upper surface | | | | | | Lower surface | | | | | |
|---|---|---|---|---|---|---|---|---|---|---|---|---|
| | x | | y | | z | | x | | y | | z | |
| | cm | in. | cm | in. | cm | in. | cm | in. | cm | in. | cm | in. |
| 1 | 32.453 | 12.777 | 4.782 | 1.883 | -3.024 | -1.191 | 32.453 | 12.777 | 4.782 | 1.883 | -3.024 | -1.191 |
| | 32.489 | 12.791 | 4.780 | 1.882 | -2.988 | -1.176 | 32.442 | 12.772 | 4.772 | 1.879 | -3.061 | -1.205 |
| | 32.573 | 12.824 | 4.783 | 1.883 | -2.959 | -1.165 | 32.502 | 12.796 | 4.771 | 1.878 | -3.082 | -1.214 |
| | 33.375 | 13.140 | 4.780 | 1.882 | -2.782 | -1.095 | 33.338 | 13.125 | 4.804 | 1.891 | -3.040 | -1.197 |
| | 38.492 | 15.154 | 4.731 | 1.862 | -1.807 | -.712 | 38.359 | 15.102 | 4.807 | 1.892 | -2.788 | -1.097 |
| | 43.541 | 17.142 | 4.730 | 1.862 | -1.154 | -.454 | 43.389 | 17.082 | 4.817 | 1.896 | -2.533 | -.997 |
| | 48.428 | 19.066 | 4.668 | 1.838 | -.829 | -.326 | 48.357 | 19.038 | 4.772 | 1.879 | -2.291 | -.902 |
| | 53.393 | 21.021 | 4.693 | 1.848 | -.803 | -.316 | 53.403 | 21.025 | 4.801 | 1.890 | -2.033 | -.800 |
| | 58.385 | 22.986 | 4.909 | 1.933 | -1.063 | -.418 | 58.421 | 23.000 | 4.801 | 1.890 | -1.780 | -.701 |
| | 60.660 | 23.882 | 4.909 | 1.933 | -1.272 | -.501 | 60.680 | 23.890 | 4.801 | 1.890 | -1.667 | -.656 |
| | 62.936 | 24.778 | 4.909 | 1.933 | -1.481 | -.583 | 62.939 | 24.779 | 4.801 | 1.890 | -1.553 | -.612 |
| | 62.938 | 24.779 | 4.909 | 1.933 | -1.507 | -.593 | 62.939 | 24.779 | 4.801 | 1.890 | -1.527 | -.601 |
| 2 | 41.609 | 16.382 | 8.535 | 3.360 | -1.901 | -0.749 | 41.609 | 16.382 | 8.535 | 3.360 | -1.901 | -0.749 |
| | 41.634 | 16.391 | 8.529 | 3.358 | -1.867 | -.735 | 41.637 | 16.393 | 8.541 | 3.363 | -1.934 | -.761 |
| | 41.703 | 16.418 | 8.525 | 3.356 | -1.840 | -.724 | 41.708 | 16.421 | 8.545 | 3.364 | -1.953 | -.769 |
| | 42.453 | 16.714 | 8.500 | 3.347 | -1.662 | -.654 | 42.466 | 16.719 | 8.546 | 3.365 | -1.921 | -.756 |
| | 45.613 | 17.958 | 8.413 | 3.312 | -1.009 | -.397 | 45.651 | 17.973 | 8.546 | 3.365 | -1.761 | -.693 |
| | 48.782 | 19.206 | 8.361 | 3.292 | -.553 | -.218 | 48.835 | 19.226 | 8.546 | 3.365 | -1.601 | -.630 |
| | 51.962 | 20.458 | 8.346 | 3.286 | -.306 | -.121 | 52.019 | 20.480 | 8.546 | 3.365 | -1.441 | -.567 |
| | 55.153 | 21.714 | 8.367 | 3.294 | -.270 | -.106 | 55.203 | 21.734 | 8.546 | 3.865 | -1.281 | -.504 |
| | 58.354 | 22.974 | 8.426 | 3.317 | -.443 | -.175 | 58.388 | 22.987 | 8.546 | 3.365 | -1.121 | -.441 |
| | 60.629 | 23.870 | 8.482 | 3.339 | -.643 | -.253 | 60.647 | 23.877 | 8.546 | 3.365 | -1.007 | -.397 |
| | 62.904 | 24.765 | 8.537 | 3.361 | -.842 | -.331 | 62.906 | 24.766 | 8.546 | 3.365 | -.894 | -.352 |
| | 62.906 | 24.766 | 8.541 | 3.363 | -.868 | -.342 | 62.906 | 24.766 | 8.541 | 3.363 | -.868 | -.342 |
| 3 | 50.478 | 19.873 | 12.170 | 4.791 | -0.814 | -0.320 | 50.478 | 19.873 | 12.170 | 4.791 | -0.814 | -0.320 |
| | 50.502 | 19.883 | 12.164 | 4.789 | -.779 | -.307 | 50.506 | 19.884 | 12.176 | 4.794 | -.846 | -.333 |
| | 50.571 | 19.910 | 12.160 | 4.788 | -.752 | -.296 | 50.577 | 19.912 | 12.180 | 4.795 | -.866 | -.341 |
| | 51.322 | 20.206 | 12.137 | 4.778 | -.583 | -.229 | 51.335 | 20.211 | 12.181 | 4.796 | -.833 | -.328 |
| | 52.714 | 20.754 | 12.094 | 4.761 | -.268 | -.106 | 52.739 | 20.763 | 12.181 | 4.796 | -.763 | -.300 |
| | 54.107 | 21.302 | 12.055 | 4.746 | .023 | .009 | 54.143 | 21.316 | 12.181 | 4.796 | -.692 | -.273 |
| | 55.506 | 21.853 | 12.036 | 4.739 | .201 | .079 | 55.547 | 21.869 | 12.181 | 4.796 | -.622 | -.245 |
| | 56.911 | 22.406 | 12.038 | 4.739 | .259 | .102 | 56.951 | 22.422 | 12.181 | 4.796 | -.551 | -.217 |
| | 58.322 | 22.961 | 12.062 | 4.749 | .197 | .077 | 58.356 | 22.975 | 12.181 | 4.796 | -.481 | -.189 |
| | 60.597 | 23.857 | 12.117 | 4.770 | -.002 | -.001 | 60.615 | 23.864 | 12.181 | 4.796 | -.367 | -.145 |
| | 62.871 | 24.753 | 12.172 | 4.792 | -.202 | -.079 | 62.874 | 24.754 | 12.181 | 4.796 | -.254 | -.100 |
| | 62.873 | 24.753 | 12.177 | 4.794 | -.228 | -.090 | 62.873 | 24.753 | 12.177 | 4.794 | -.228 | -.090 |

TABLE I.- Concluded

(c) Vertical tail coordinates

| Chord | x | | y | | z | |
|---|---|---|---|---|---|---|
| | cm | in. | cm | in. | cm | in. |
| 1 | 48.357 | 19.038 | 0.000 | 0.000 | 2.840 | 1.118 |
| | 48.357 | 19.038 | .023 | .009 | 2.836 | 1.117 |
| | 48.366 | 19.042 | .043 | .017 | 2.833 | 1.115 |
| | 48.382 | 19.048 | .057 | .022 | 2.831 | 1.115 |
| | 48.403 | 19.056 | .063 | .025 | 2.831 | 1.115 |
| | 50.857 | 20.023 | .307 | .121 | 2.854 | 1.124 |
| | 53.320 | 20.992 | .552 | .217 | 2.874 | 1.131 |
| | 55.751 | 21.949 | .796 | .313 | 2.873 | 1.131 |
| | 57.721 | 22.725 | 1.016 | .400 | 2.679 | 1.055 |
| | 57.722 | 22.725 | .000 | .000 | 2.679 | 1.055 |
| 2 | 48.735 | 19.187 | 0.000 | 0.000 | 3.157 | 1.243 |
| | 48.739 | 19.189 | .023 | .009 | 3.157 | 1.243 |
| | 48.752 | 19.194 | .043 | .017 | 3.157 | 1.243 |
| | 48.770 | 19.201 | .057 | .022 | 3.157 | 1.243 |
| | 48.792 | 19.210 | .063 | .025 | 3.157 | 1.243 |
| | 51.309 | 20.200 | .316 | .125 | 3.157 | 1.243 |
| | 53.826 | 21.191 | .570 | .224 | 3.157 | 1.243 |
| | 56.342 | 22.182 | .823 | .324 | 3.157 | 1.243 |
| | 58.859 | 23.173 | 1.076 | .424 | 3.157 | 1.243 |
| | 58.860 | 23.173 | .000 | .000 | 3.157 | 1.243 |
| 3 | 50.133 | 19.737 | 0.000 | 0.000 | 4.330 | 1.705 |
| | 50.137 | 19.739 | .023 | .009 | 4.330 | 1.705 |
| | 50.149 | 19.744 | .043 | .017 | 4.330 | 1.705 |
| | 50.167 | 19.751 | .057 | .022 | 4.330 | 1.705 |
| | 50.190 | 19.760 | .063 | .025 | 4.330 | 1.705 |
| | 53.054 | 20.888 | .353 | .139 | 4.330 | 1.705 |
| | 55.919 | 22.015 | .644 | .253 | 4.330 | 1.705 |
| | 58.784 | 23.143 | .934 | .368 | 4.330 | 1.705 |
| | 61.648 | 24.271 | 1.224 | .482 | 4.330 | 1.705 |
| | 61.649 | 24.271 | .000 | .000 | 4.330 | 1.705 |

| Chord | x | | y | | z | |
|---|---|---|---|---|---|---|
| | cm | in. | cm | in. | cm | in. |
| 4 | 54.126 | 21.309 | 0.000 | 0.000 | 7.681 | 3.024 |
| | 54.130 | 21.311 | .023 | .009 | 7.681 | 3.024 |
| | 54.142 | 21.316 | .043 | .017 | 7.681 | 3.024 |
| | 54.161 | 21.323 | .057 | .022 | 7.681 | 3.024 |
| | 54.183 | 21.332 | .063 | .025 | 7.681 | 3.024 |
| | 56.313 | 22.170 | .275 | .108 | 7.681 | 3.024 |
| | 58.443 | 23.009 | .487 | .192 | 7.681 | 3.024 |
| | 60.573 | 23.848 | .700 | .275 | 7.681 | 3.024 |
| | 62.703 | 24.686 | .912 | .359 | 7.681 | 3.024 |
| | 62.704 | 24.686 | .000 | .000 | 7.681 | 3.024 |
| 5 | 58.119 | 22.881 | 0.000 | 0.000 | 11.031 | 4.343 |
| | 58.123 | 22.883 | .023 | .009 | 11.031 | 4.343 |
| | 58.135 | 22.888 | .043 | .017 | 11.031 | 4.343 |
| | 58.154 | 22.895 | .057 | .022 | 11.031 | 4.343 |
| | 58.176 | 22.904 | .063 | .025 | 11.031 | 4.343 |
| | 59.572 | 23.453 | .197 | .078 | 11.031 | 4.343 |
| | 60.967 | 24.003 | .331 | .130 | 11.031 | 4.343 |
| | 62.362 | 24.552 | .465 | .183 | 11.031 | 4.343 |
| | 63.757 | 25.101 | .599 | .236 | 11.031 | 4.343 |
| | 63.758 | 25.101 | .000 | .000 | 11.031 | 4.343 |

TABLE II.- GEOMETRIC CHARACTERISTICS OF MODEL

| | |
|---|---|
| **Wing:** | |
| Area (includes fuselage intercept), $m^2$ ($in^2$) | 0.060 (92.63) |
| Area, exposed, $m^2$ ($in^2$) | 0.030 (47.00) |
| Area, wetted, $m^2$ ($in^2$) | 0.064 (98.98) |
| Span, m (in.) | 0.244 (9.62) |
| Aspect ratio | 0.999 |
| Root chord (at fuselage center line), m (in.) | 0.371 (14.59) |
| Tip chord, m (in.) | 0.119 (4.7) |
| Taper ratio | 0.322 |
| Mean aerodynamic chord (includes fuselage intercept), m (in.) | 0.294 (11.57) |
| Sweepback angles: | |
| Leading edge, deg | 67.5 |
| 25-percent chord line, deg | 61.1 |
| Trailing edge, deg | 0 |
| Dihedral angle, deg | 10 |
| Incidence angle, deg | -2.1 |
| Airfoil thickness ratio: | |
| Exposed root | 0.051 |
| Tip | 0.078 |
| Leading-edge radius (normal to leading edge), cm (in.) | 0.064 (0.025) |
| Trailing-edge thickness, cm (in.) | 0.064 (0.025) |
| Elevons: | |
| Tip chord, percent wing tip | 36.6 |
| Span, percent total span | 59.8 |
| Area, both, $m^2$ ($in^2$) | 0.0064 (9.89) |
| **Vertical tail:** | |
| Area, exposed, $m^2$ ($in^2$) | 0.007 (10.93) |
| Span, exposed, m (in.) | 0.077 (3.06) |
| Aspect ratio of exposed area | 0.857 |
| Root chord at fuselage surface line, m (in.) | 0.101 (3.99) |
| Tip chord, m (in.) | 0.057 (2.256) |
| Taper ratio | 0.565 |
| Mean aerodynamic chord of exposed area, m (in.) | 0.097 (3.804) |
| Sweepback angles: | |
| Leading edge, deg | 49.9 |
| Trailing edge, deg | 18.5 |
| Hinge line location, percent chord | 68.7 |
| $A_{rudder}/A_{total}$ | 0.295 |
| Leading-edge radius, cm (in.) | 0.064 (0.025) |
| **Fuselage:** | |
| Length, m (in.) | 0.584 (23.0) |
| Nose radius, cm (in.) | 0.159 (0.063) |
| Maximum height, m (in.) | 0.076 (2.98) |
| Maximum width, m (in.) | 0.097 (3.83) |
| Fineness ratio of equivalent round body | 6.86 |
| Planform area, $m^2$ ($in^2$) | 0.042 (65.12) |
| Wetted area: | |
| Without components or base, $m^2$ ($in^2$) | 0.122 (188.6) |
| With wing on, $m^2$ ($in^2$) | 0.116 (179.4) |
| $A_b$, $m^2$ ($in^2$) | 0.0023 (3.54) |
| **Complete model:** | |
| Planform area, $m^2$ ($in^2$) | 0.072 (112.12) |
| Aspect ratio of planform | 0.825 |

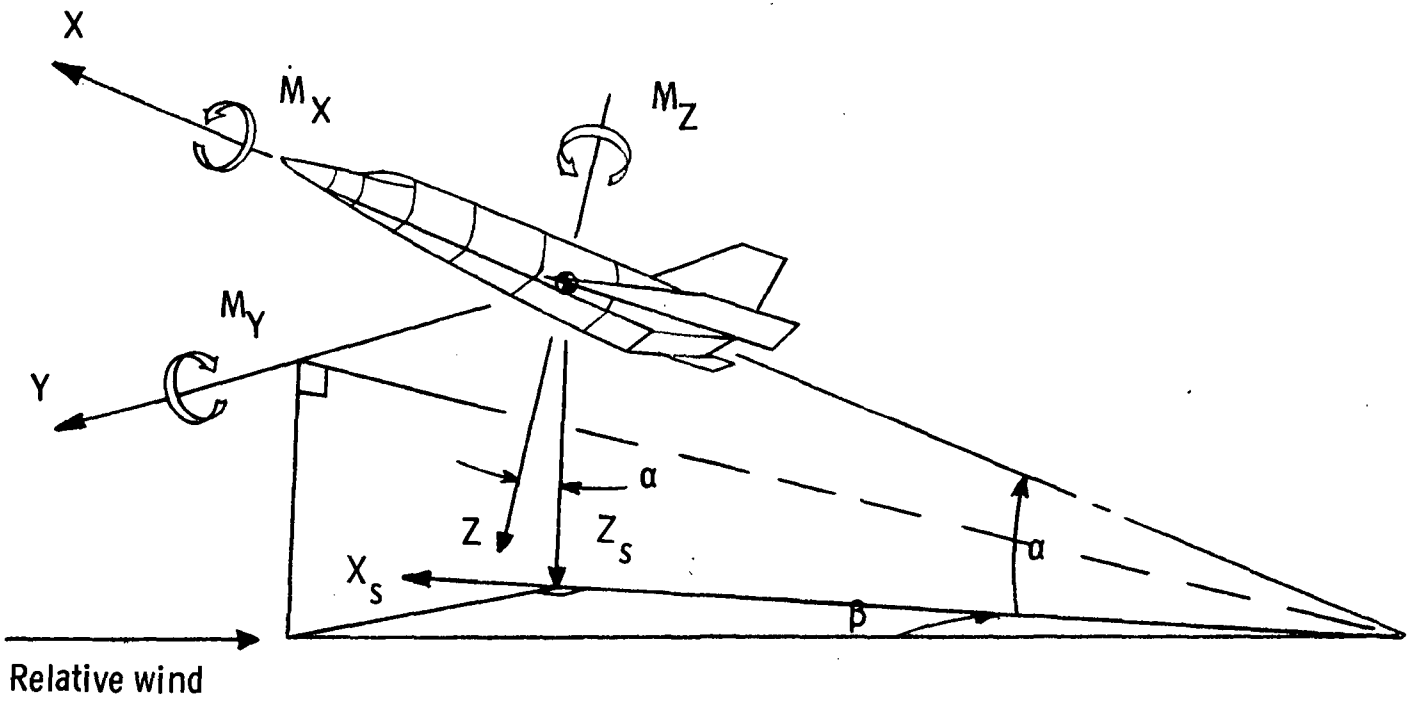


Figure 1.- System of reference axes. Arrows indicate positive directions.

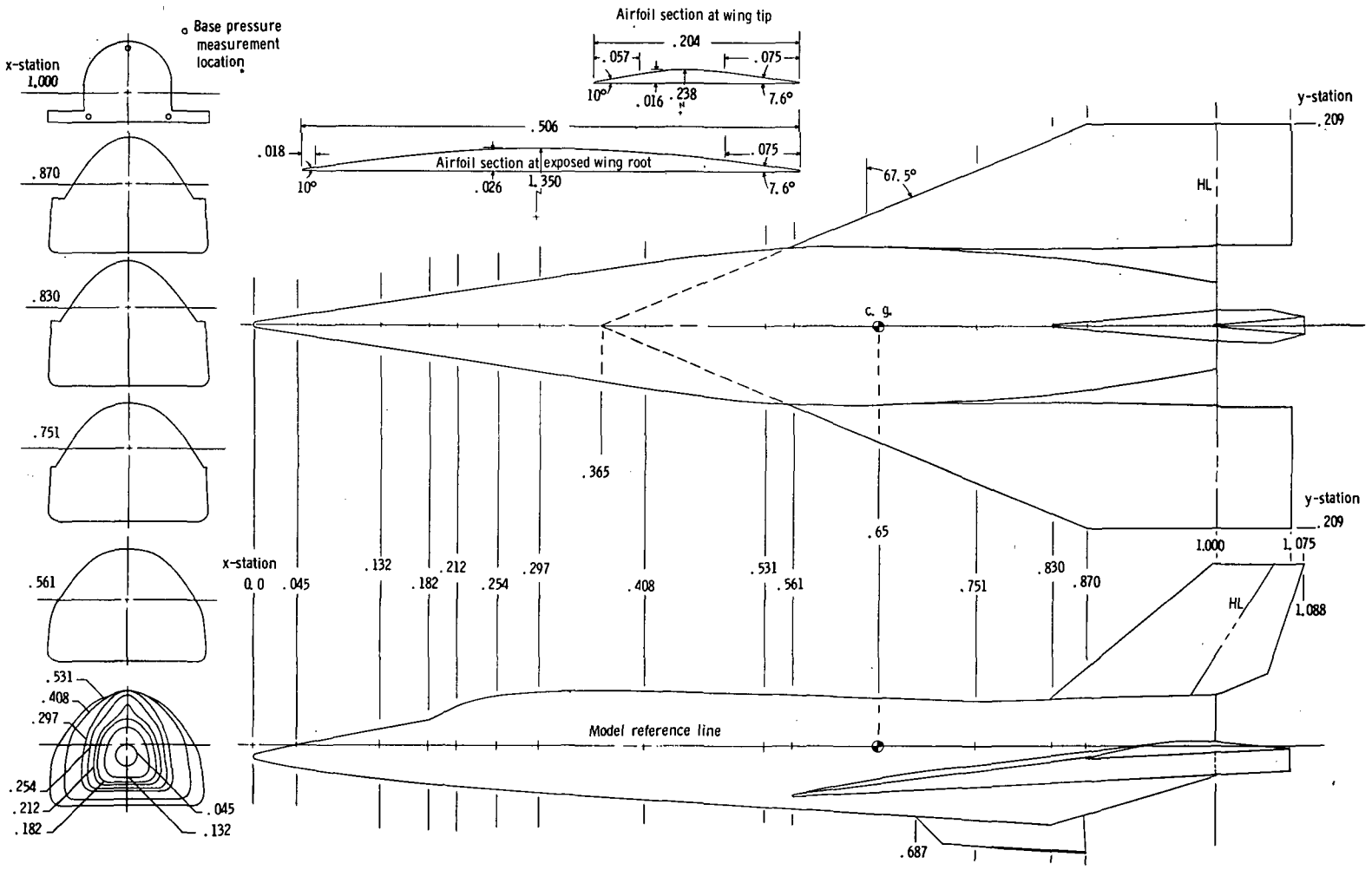


(a) Model details

Figure 2.- Model general dimensions. All dimensions have been normalized by body length ($\ell$ = 58.4 cm).

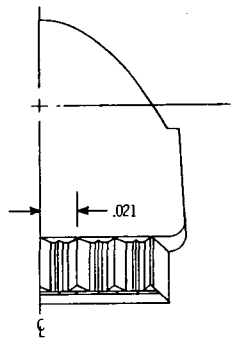


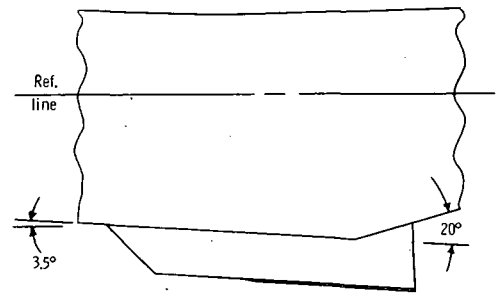


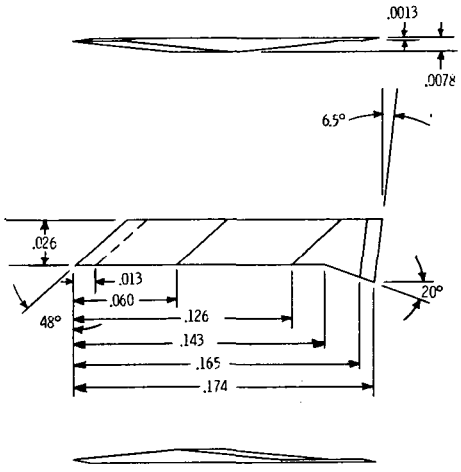


Left outside plate

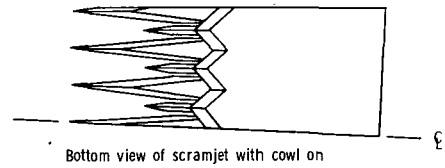


Bottom view of scramjet with cowl on

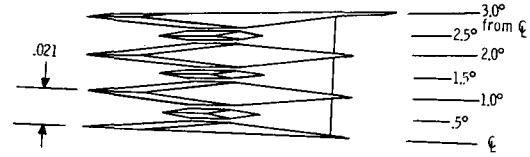


Bottom view of scramjet with cowl off

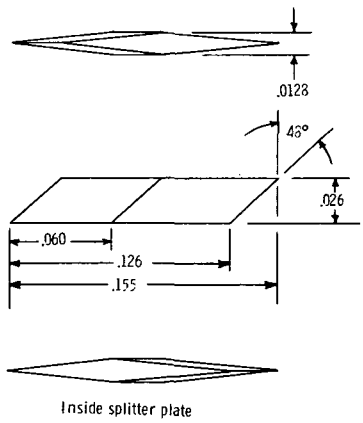


Inside splitter plate

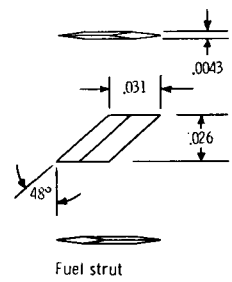


Fuel strut

(b) Scramjet engine details.

Figure 2.- Continued.

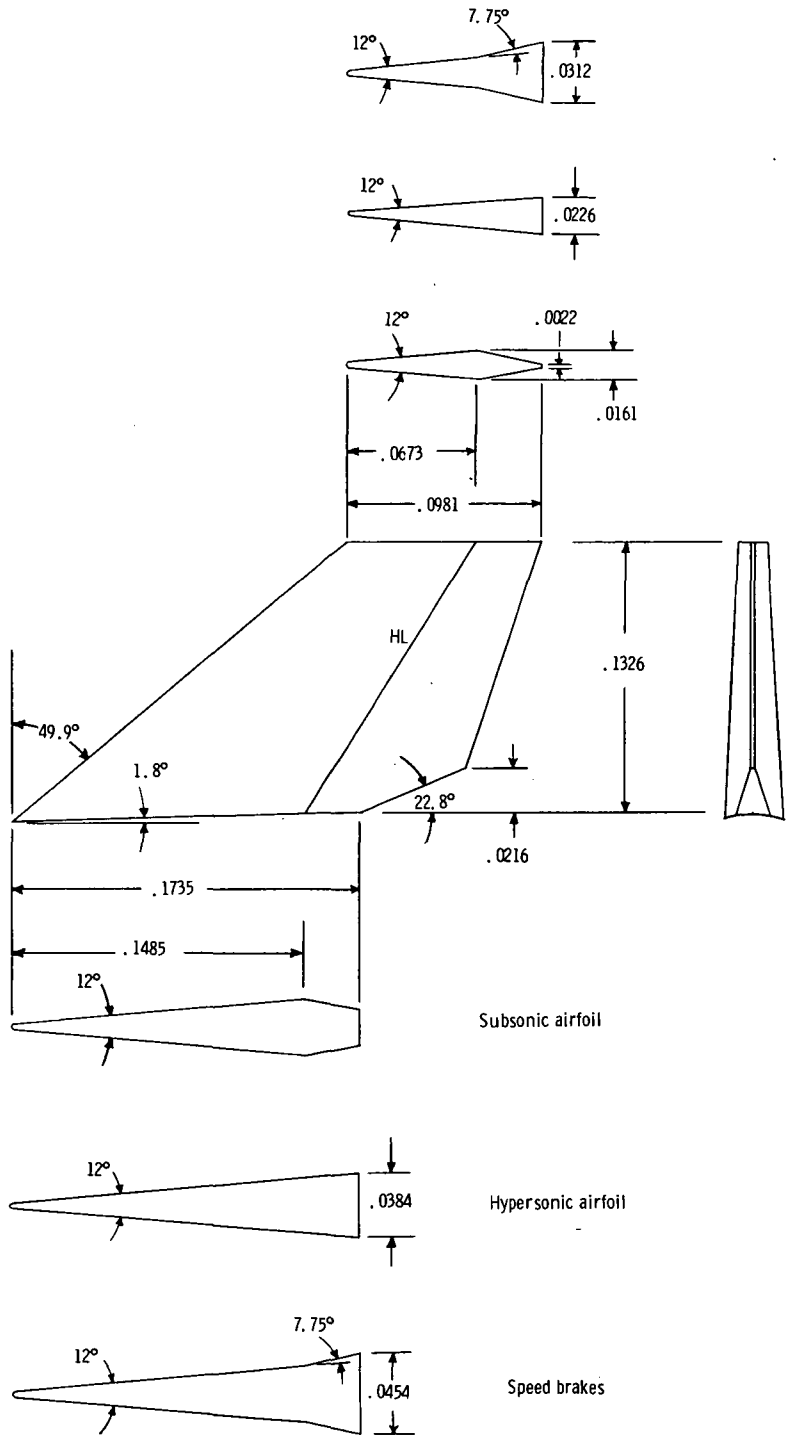


(c) Vertical tail variations.

Figure 2.- Concluded.

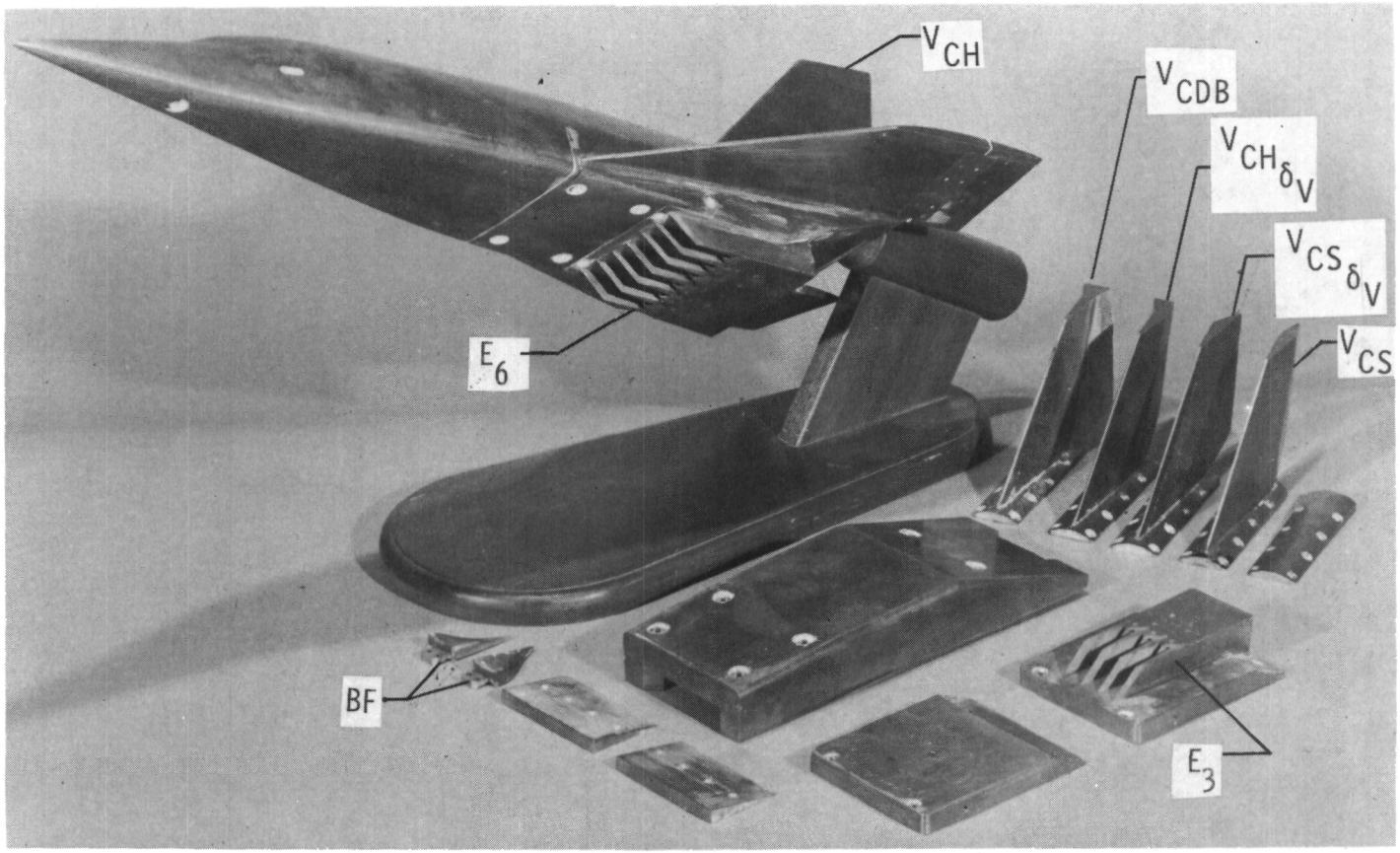


L-76-6977.2

Figure 3.- Photograph of model with various parts. (Note that all components were not used in this test.)

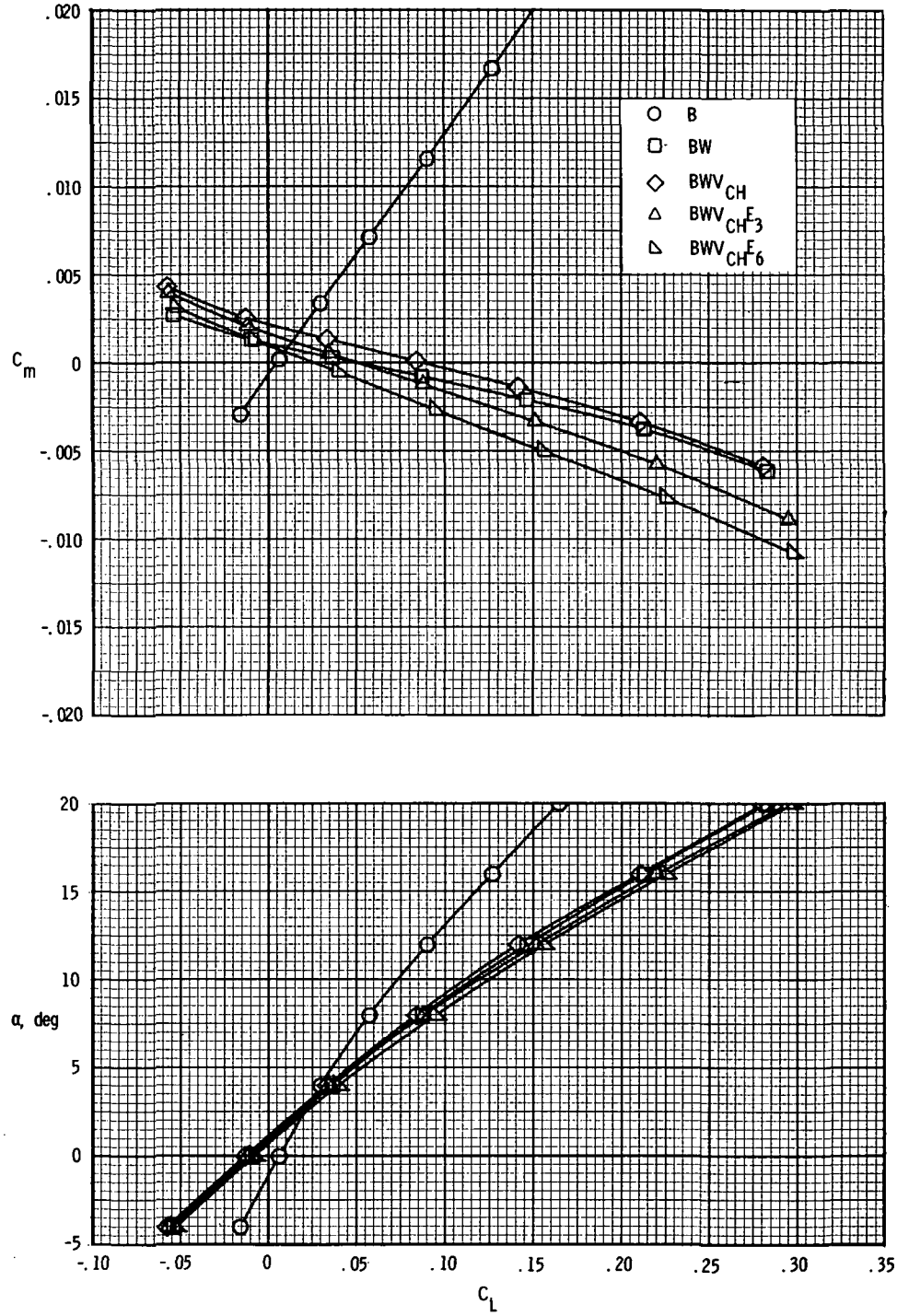


Figure 4.- Effect of body buildup on untrimmed longitudinal aerodynamic characteristics.

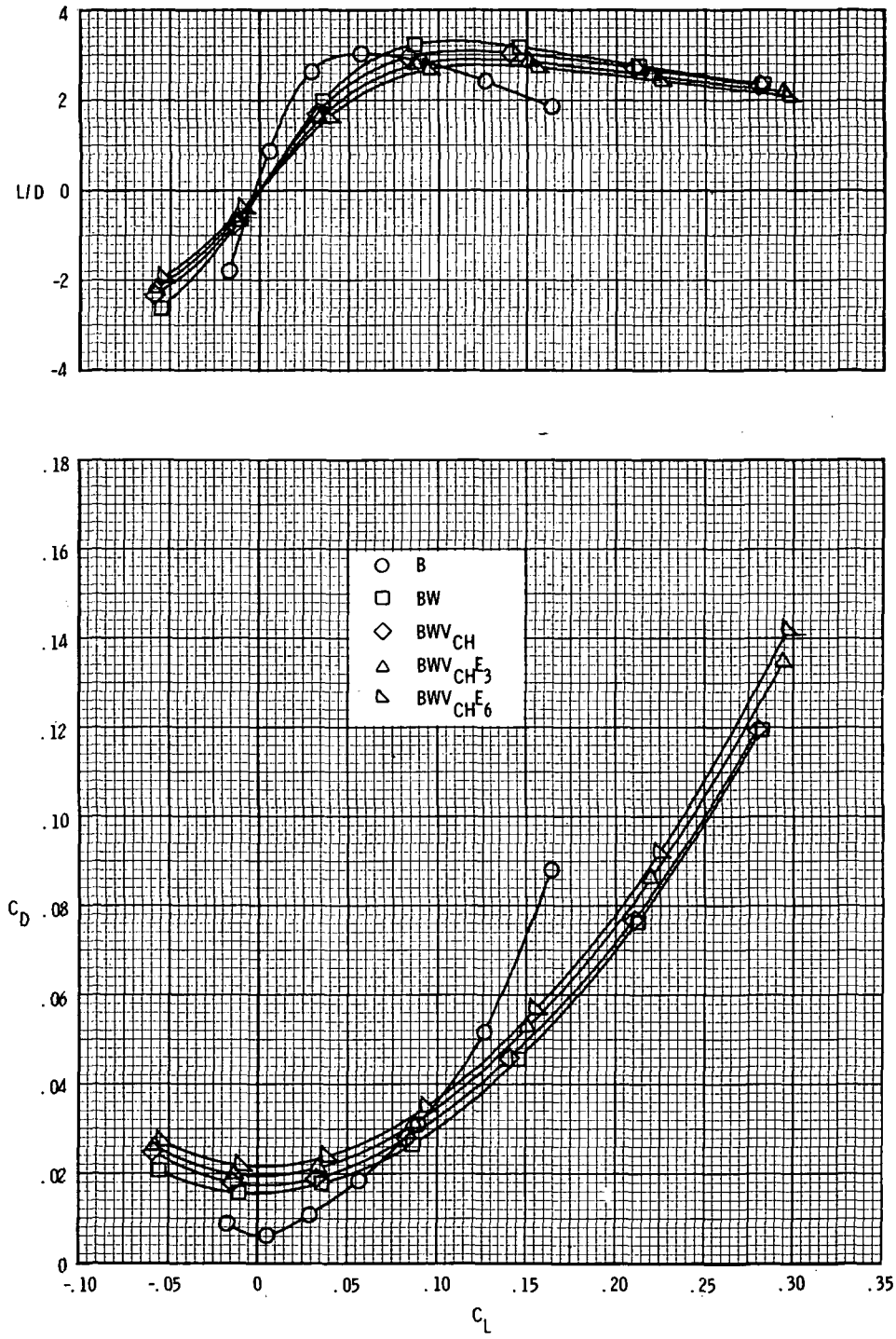


Figure 4.- Concluded.

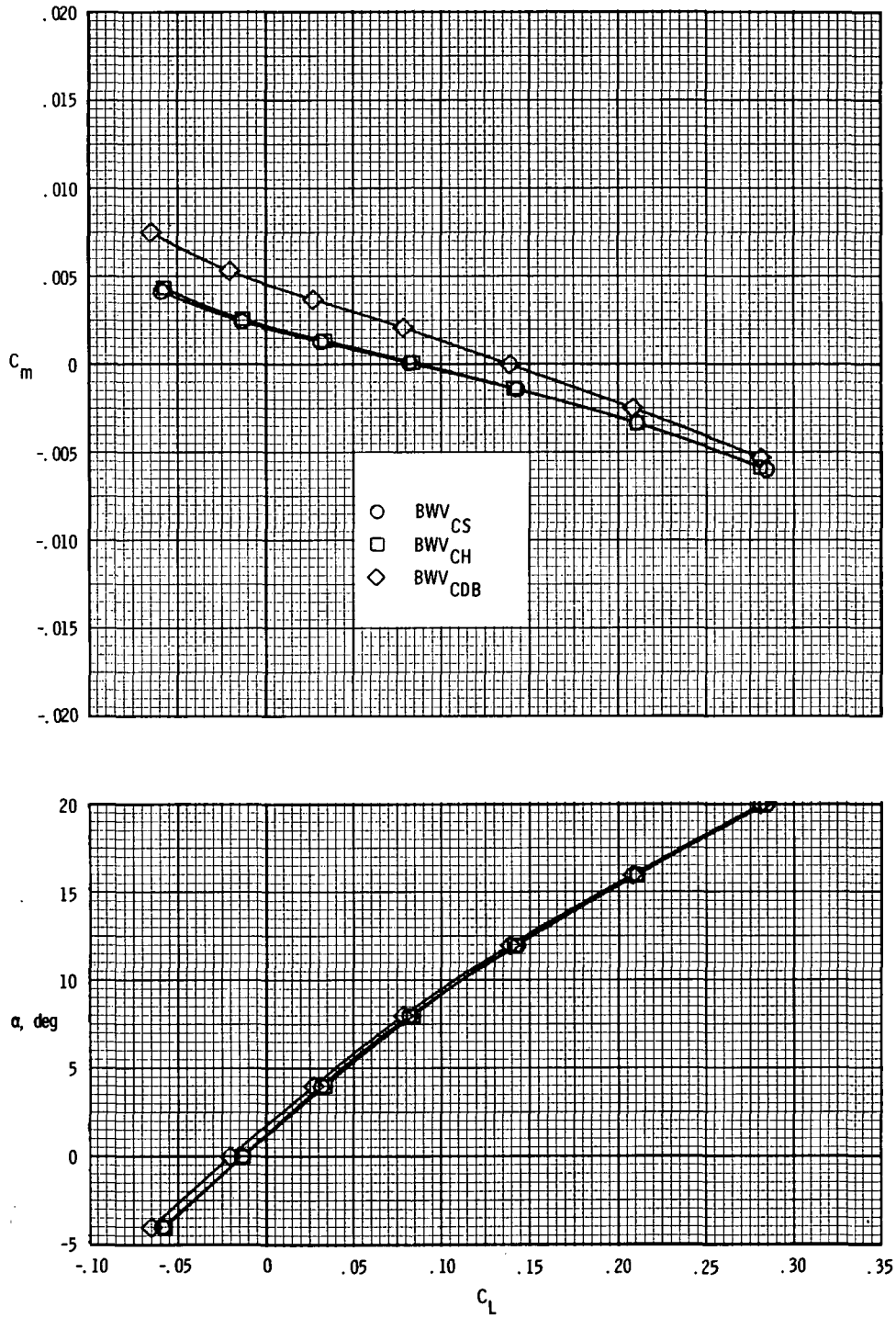


Figure 5.- Effect of vertical-tail variations on longitudinal aerodynamic characteristics of basic configuration $(BWV_{CH})$.

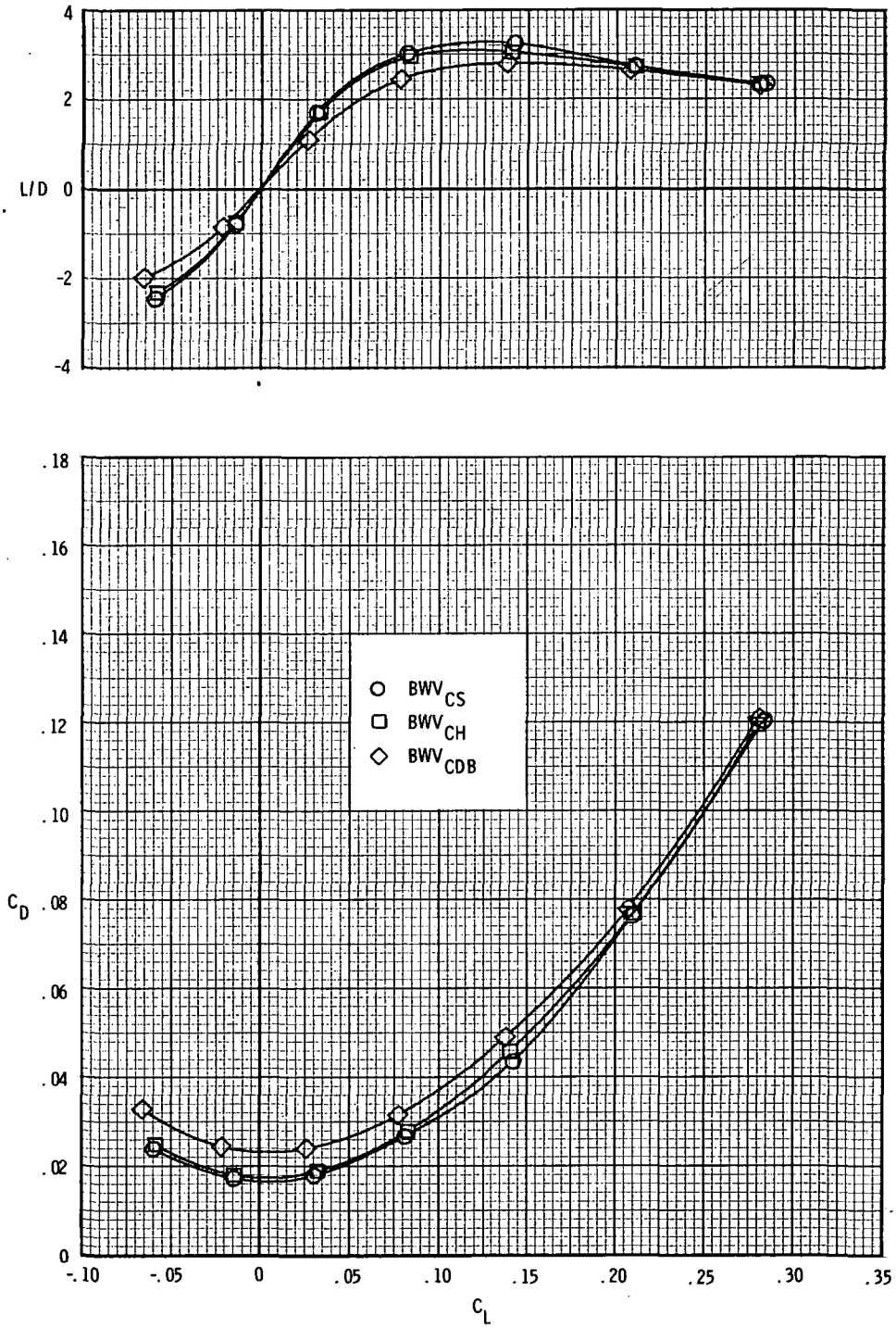


Figure 5.- Concluded.

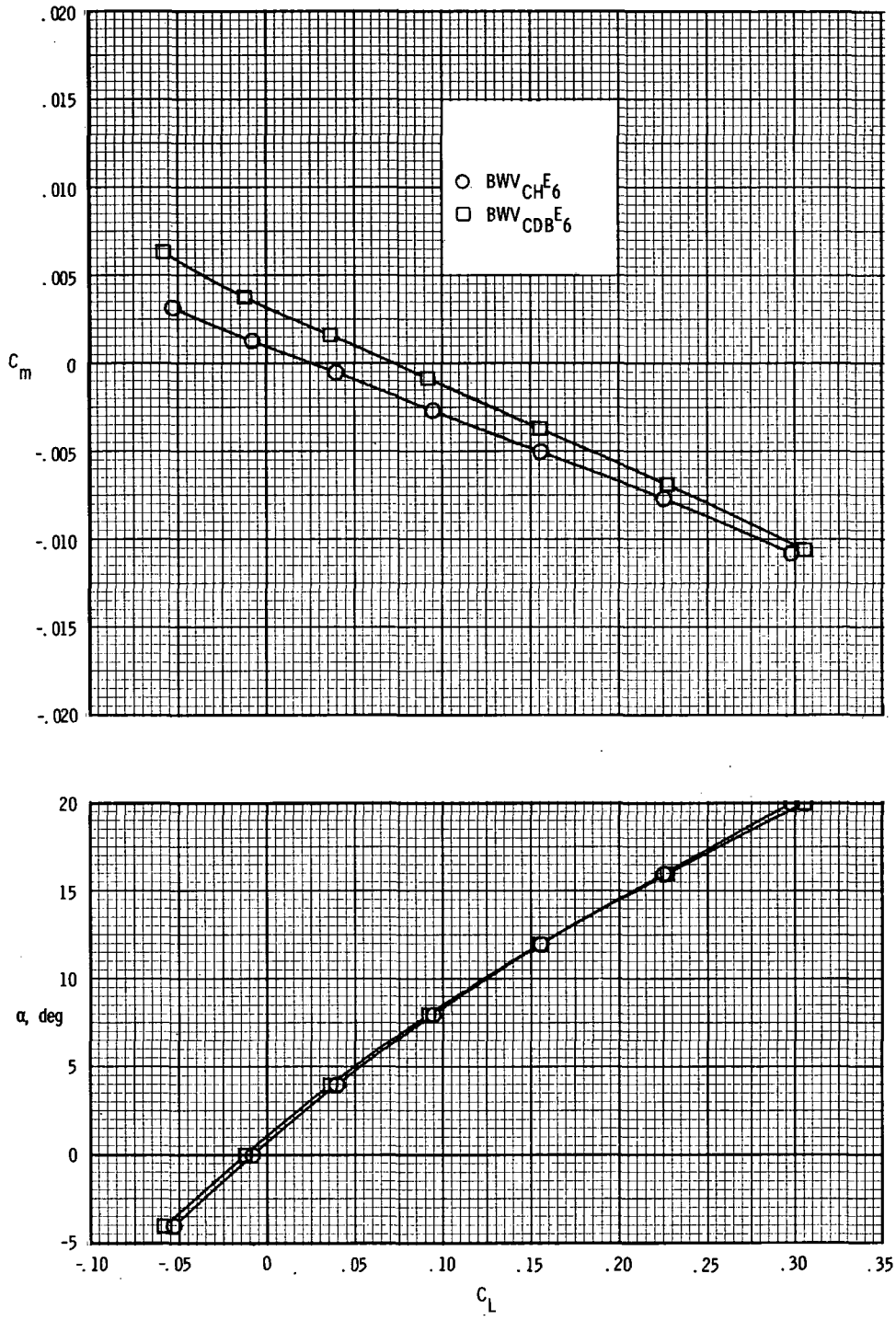


Figure 6.- Effect of speed brakes on longitudinal aerodynamic characteristics of complete configuration $\left(BWV_{CH}E_6\right)$.

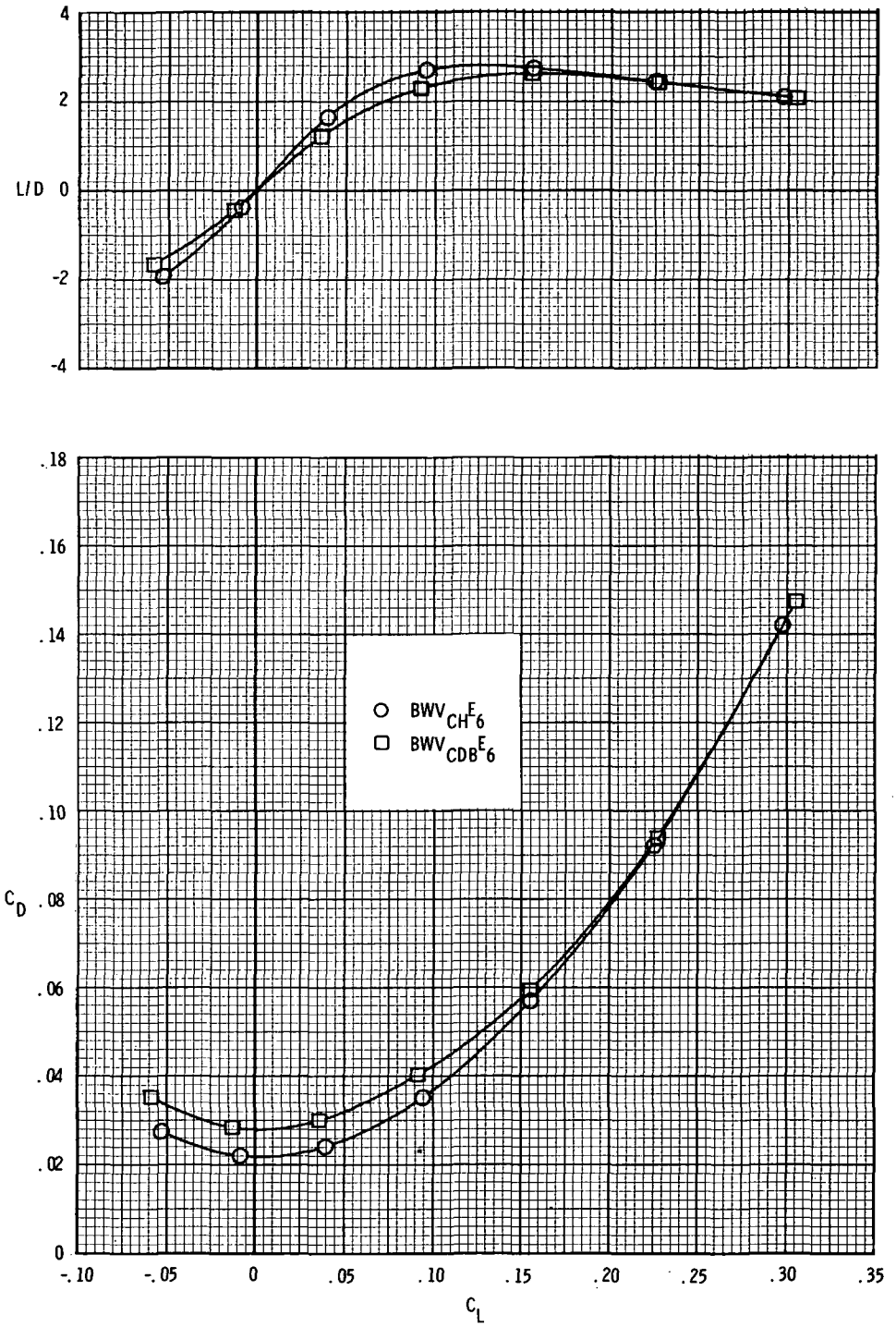


Figure 6.- Concluded.

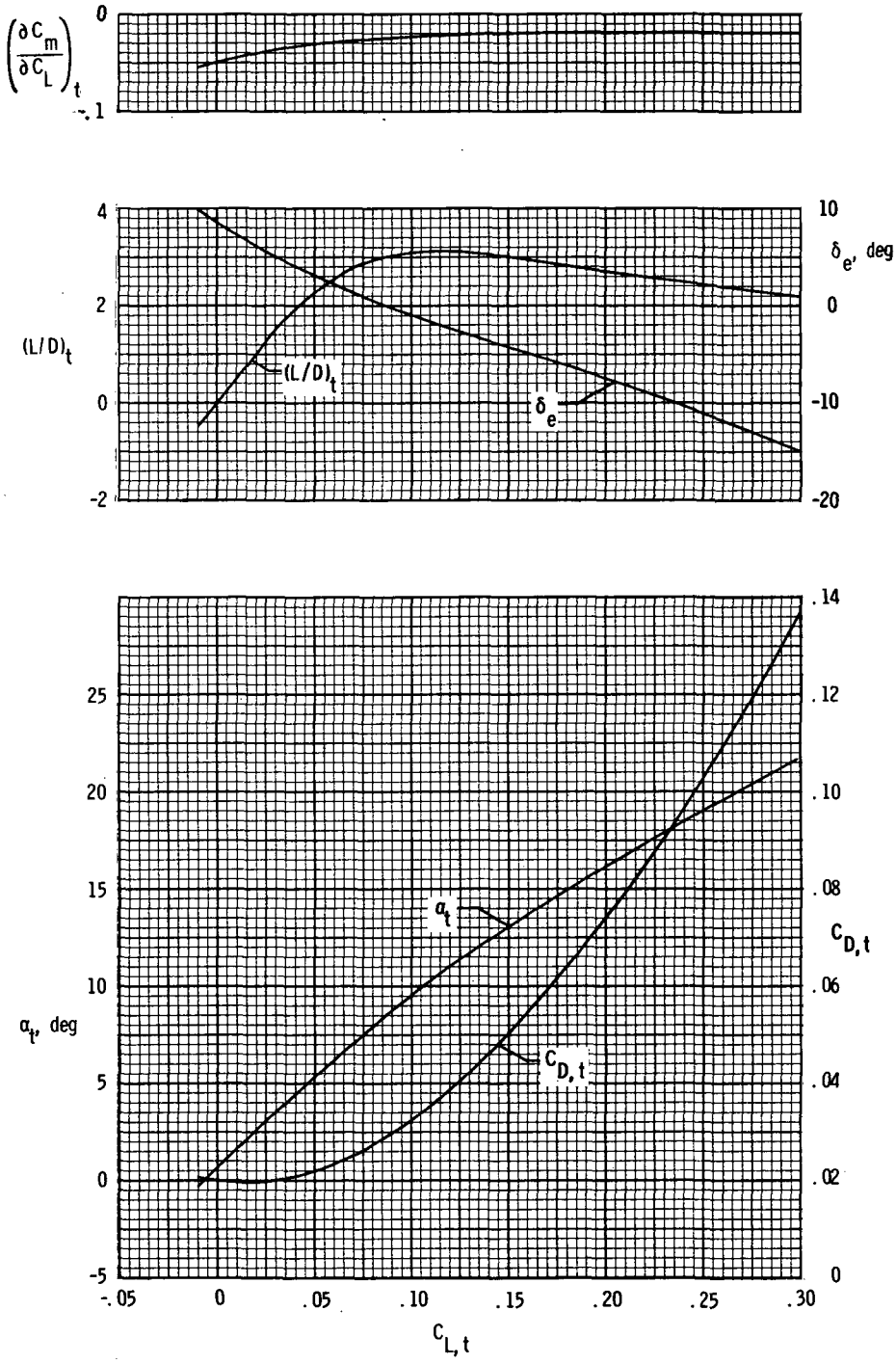


Figure 7.- Trimmed longitudinal aerodynamic characteristics of basic configuration $(BWV_{CH})$.

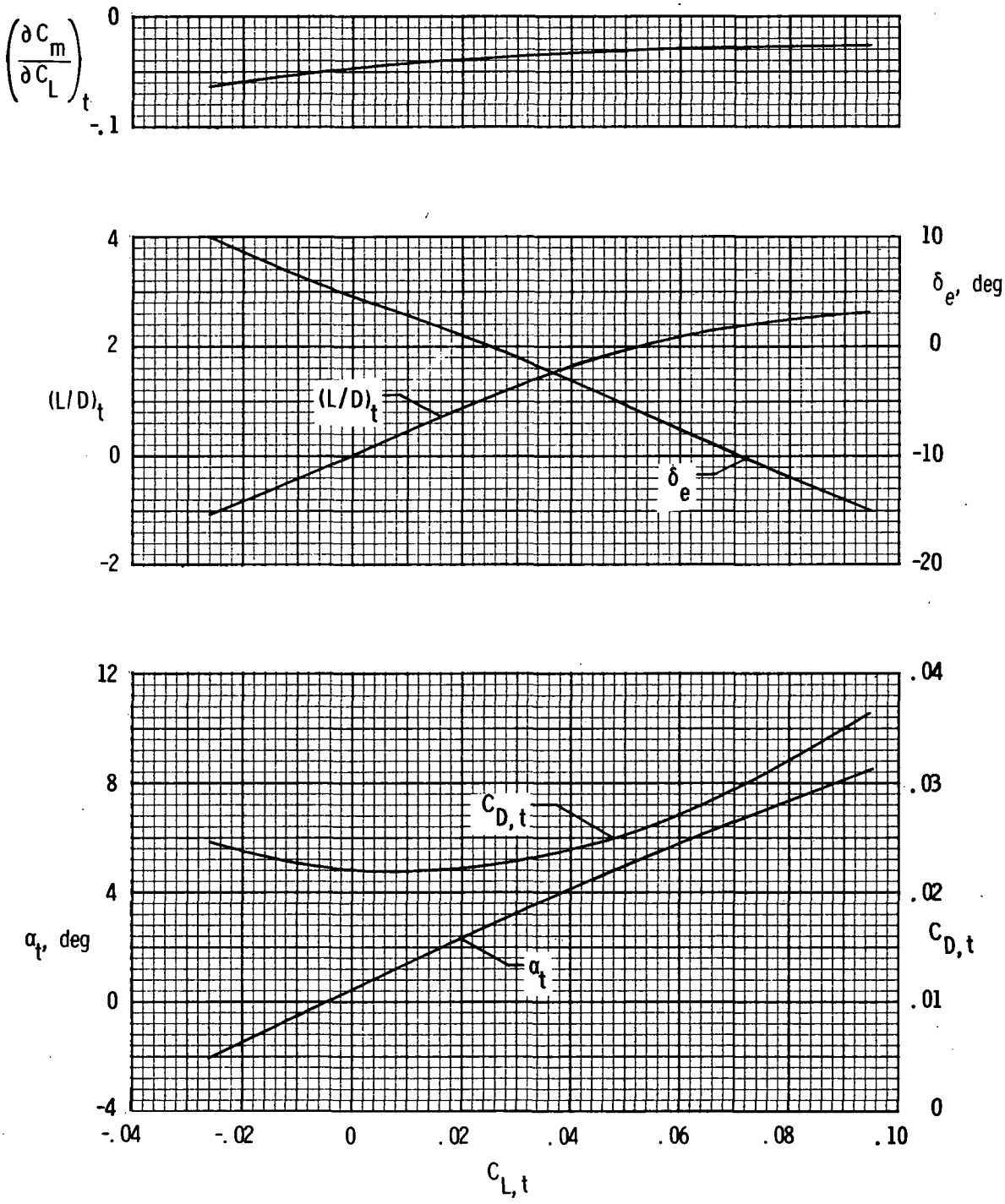


Figure 8.- Trimmed longitudinal aerodynamic characteristics of complete configuration $(BWV_{CH}E_6)$.

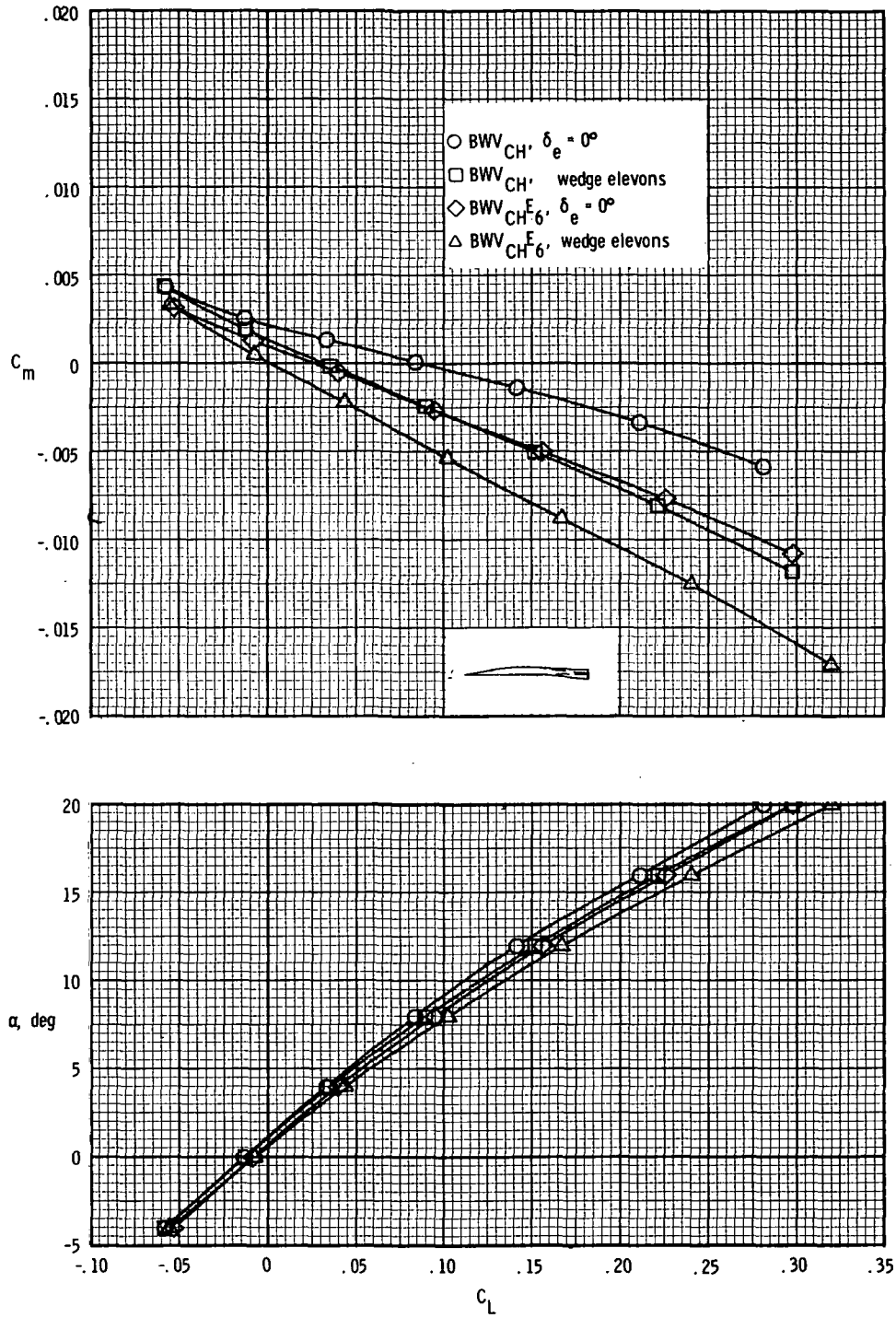


Figure 9.- Effect of wedge elevons on longitudinal aerodynamic characteristics of $BWV_{CH}$ and $BWV_{CH}E_6$ configurations.

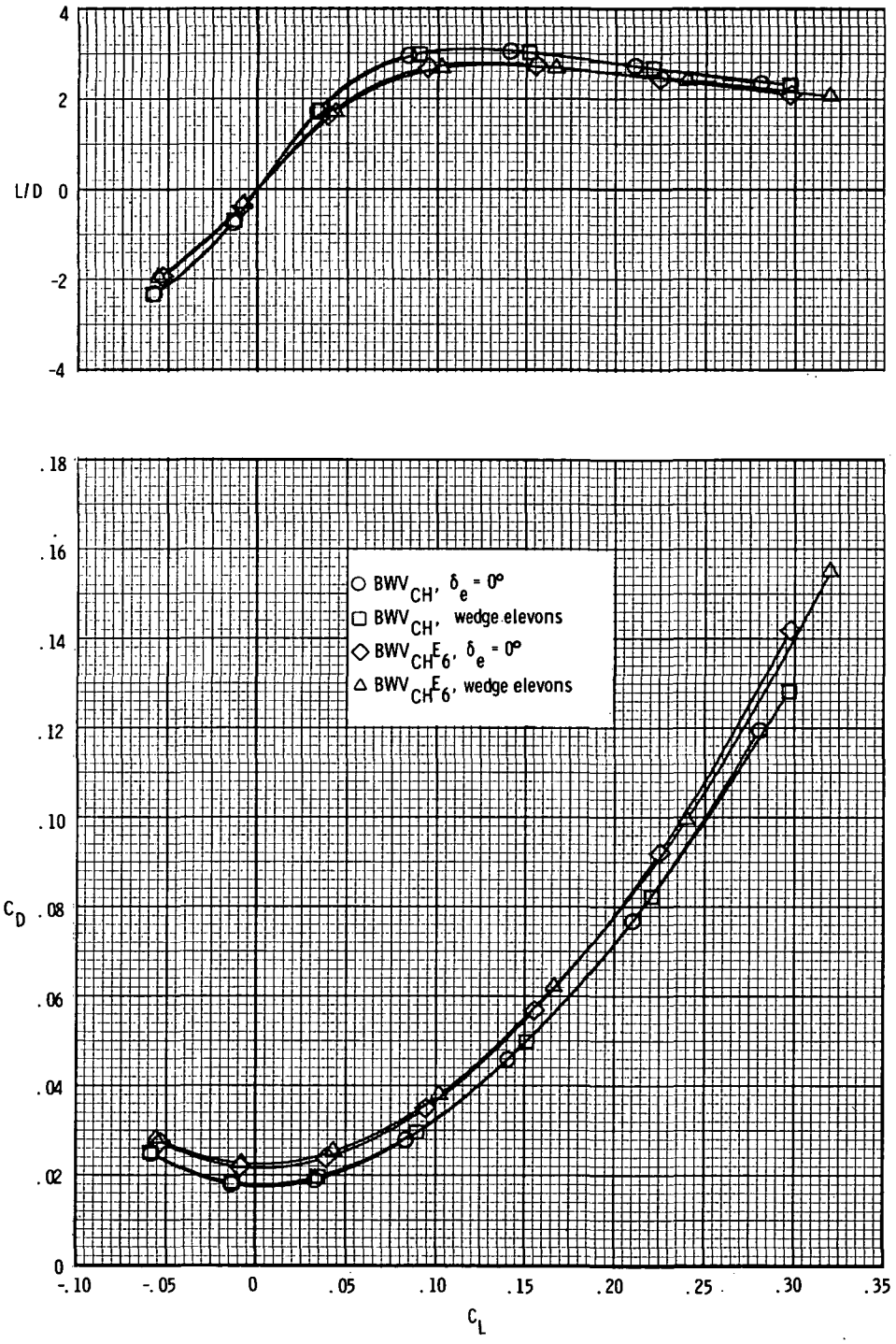


Figure 9.- Concluded.

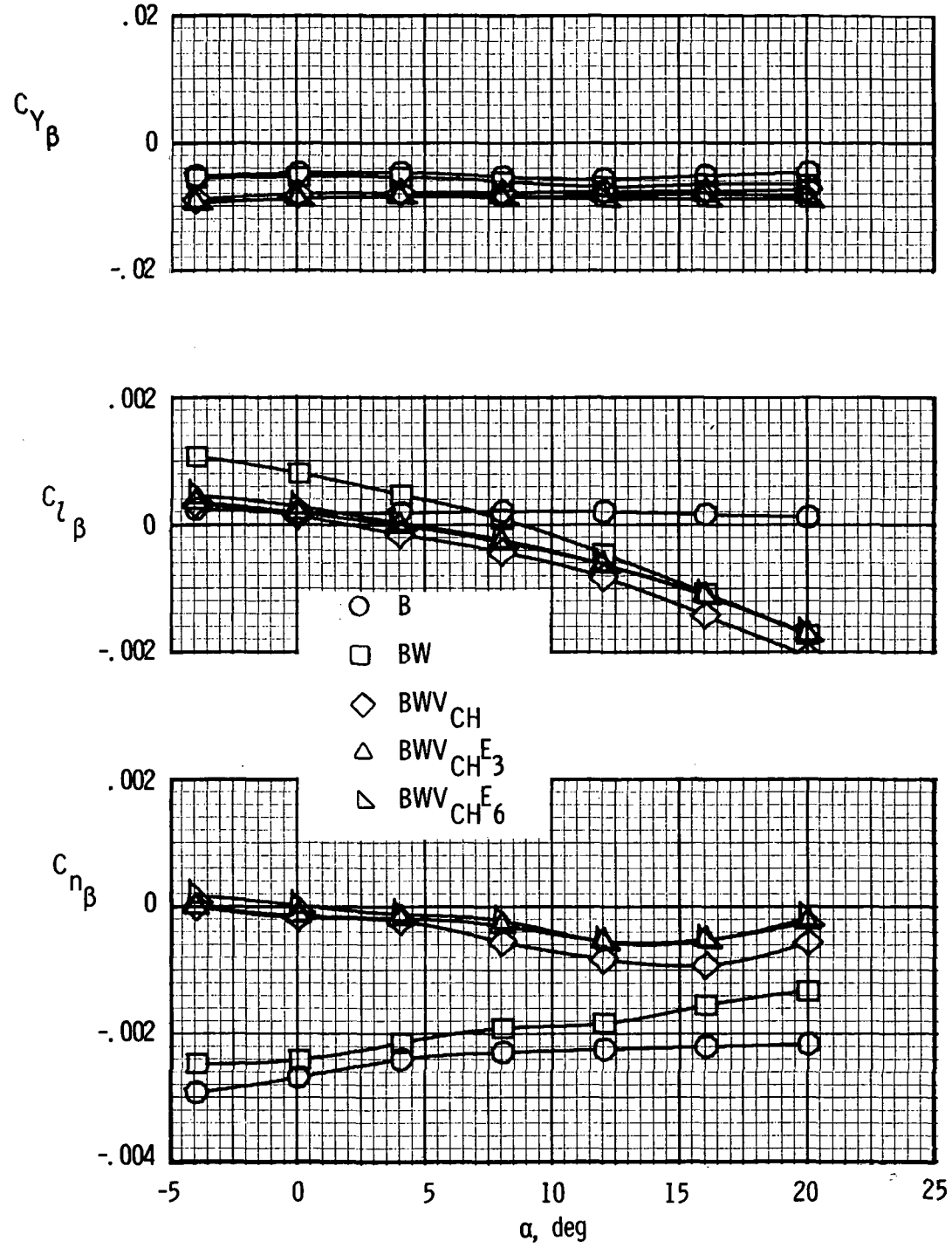


Figure 10.- Effect of body buildup on static lateral-directional stability characteristics. $\Delta\beta = -2^{o}$.

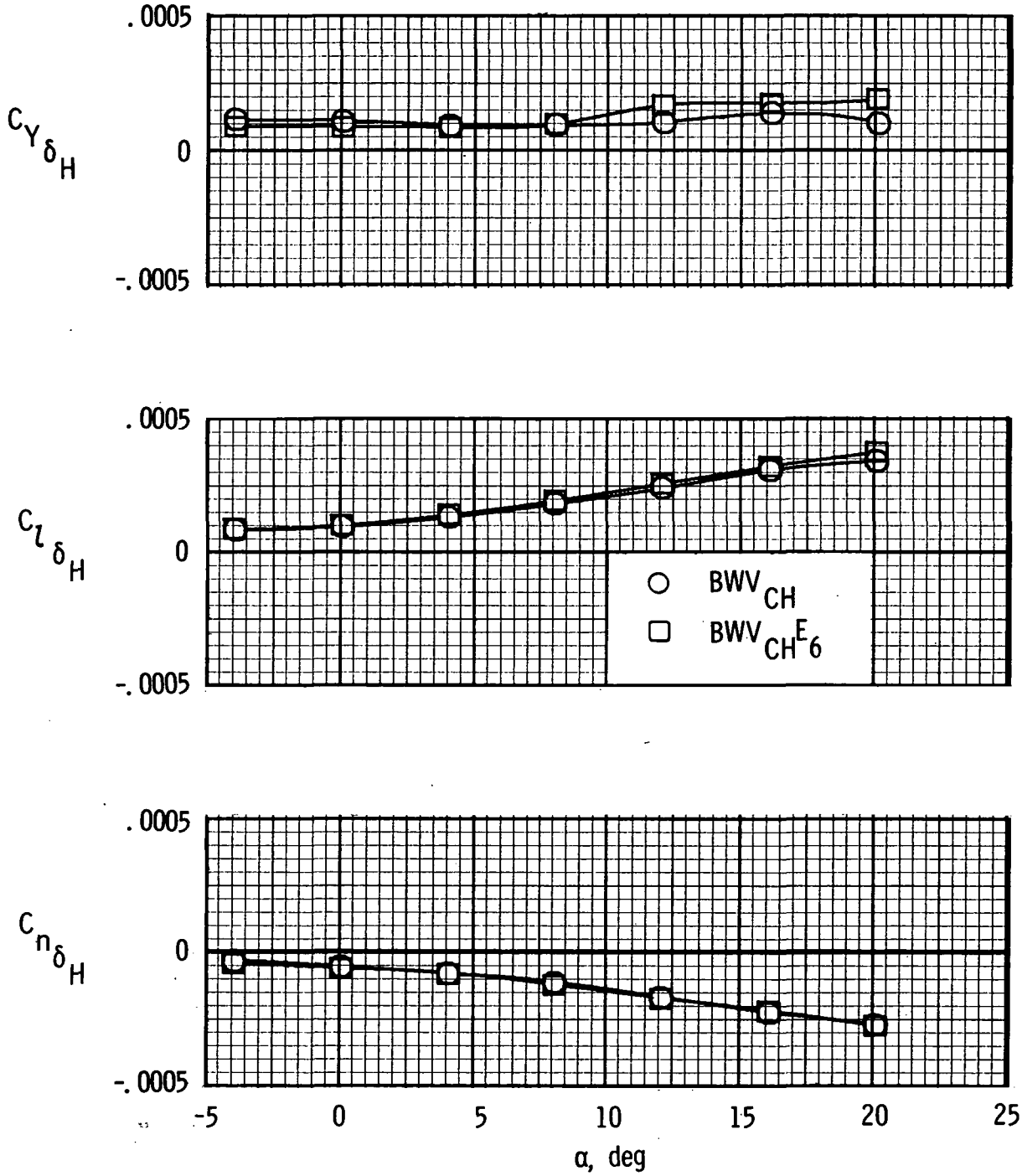


Figure 11.- Roll control characteristics for basic $(BWV_{CH})$ and complete $(BWV_{CH}E_6)$ configurations.

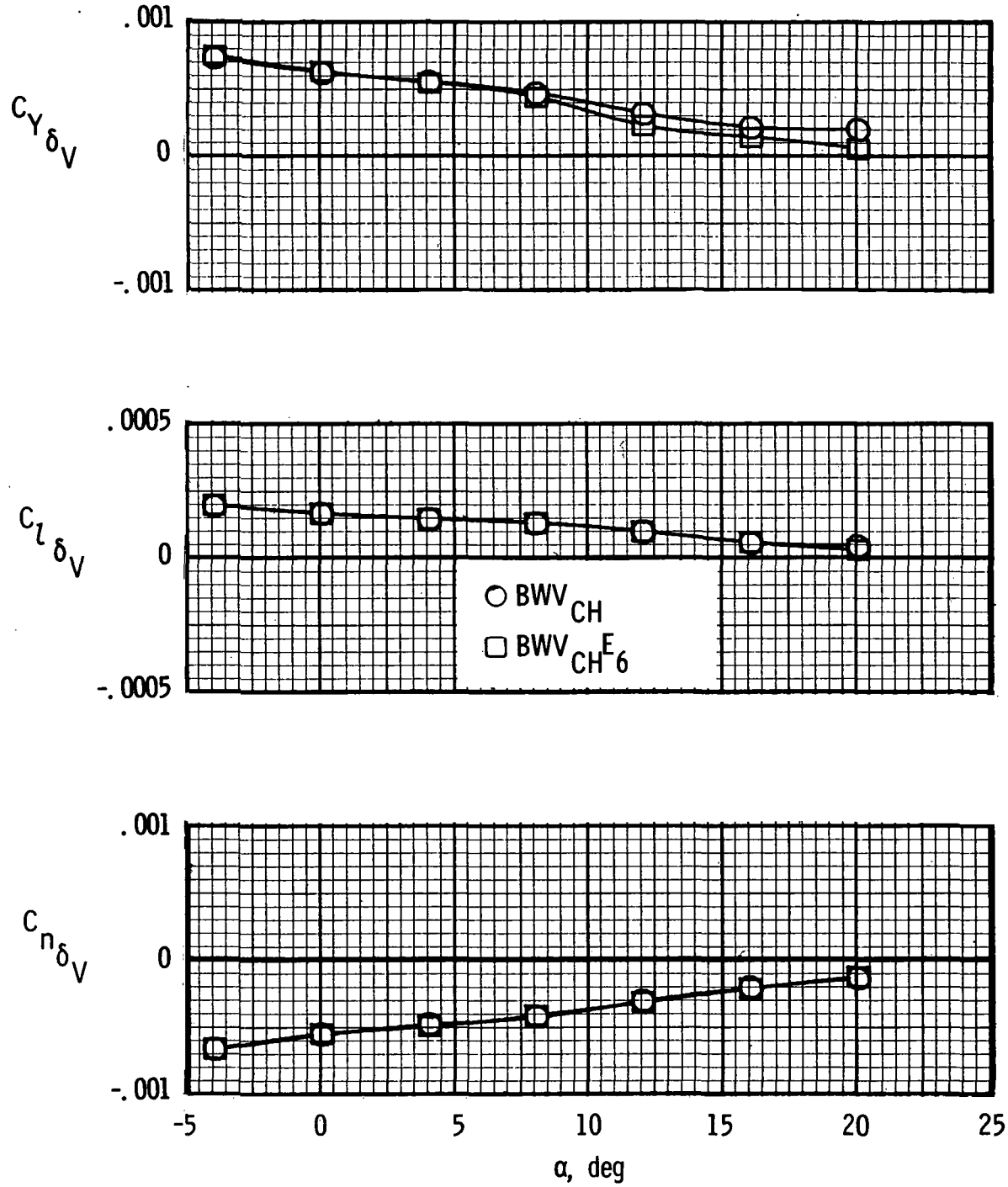


Figure 12.- Yaw control characteristics for basic $(BWV_{CH})$ and complete $(BWV_{CH}E_6)$ configurations.

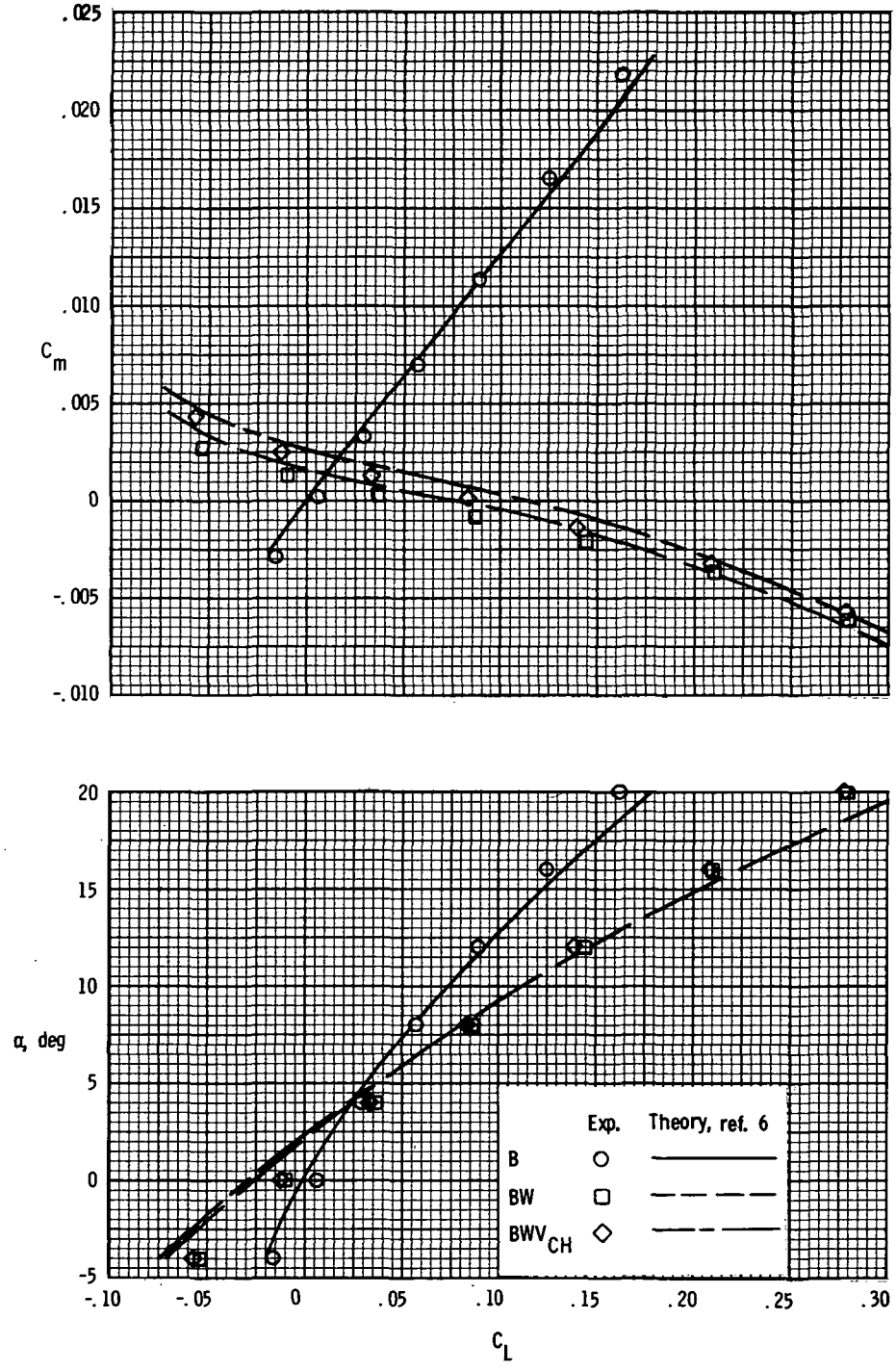


Figure 13.- Comparison of experiment with theory for body buildup.

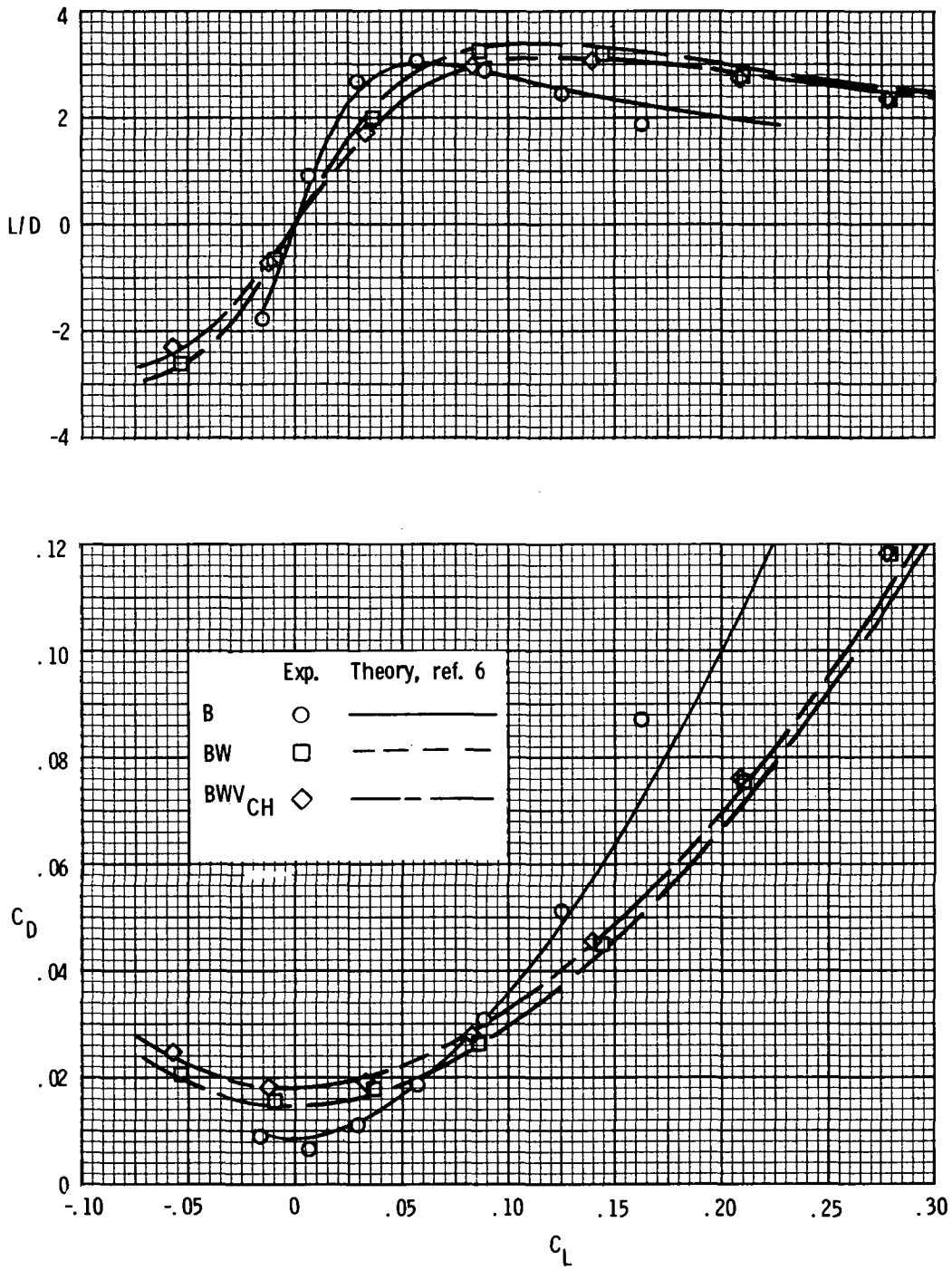


Figure 13.- Concluded.

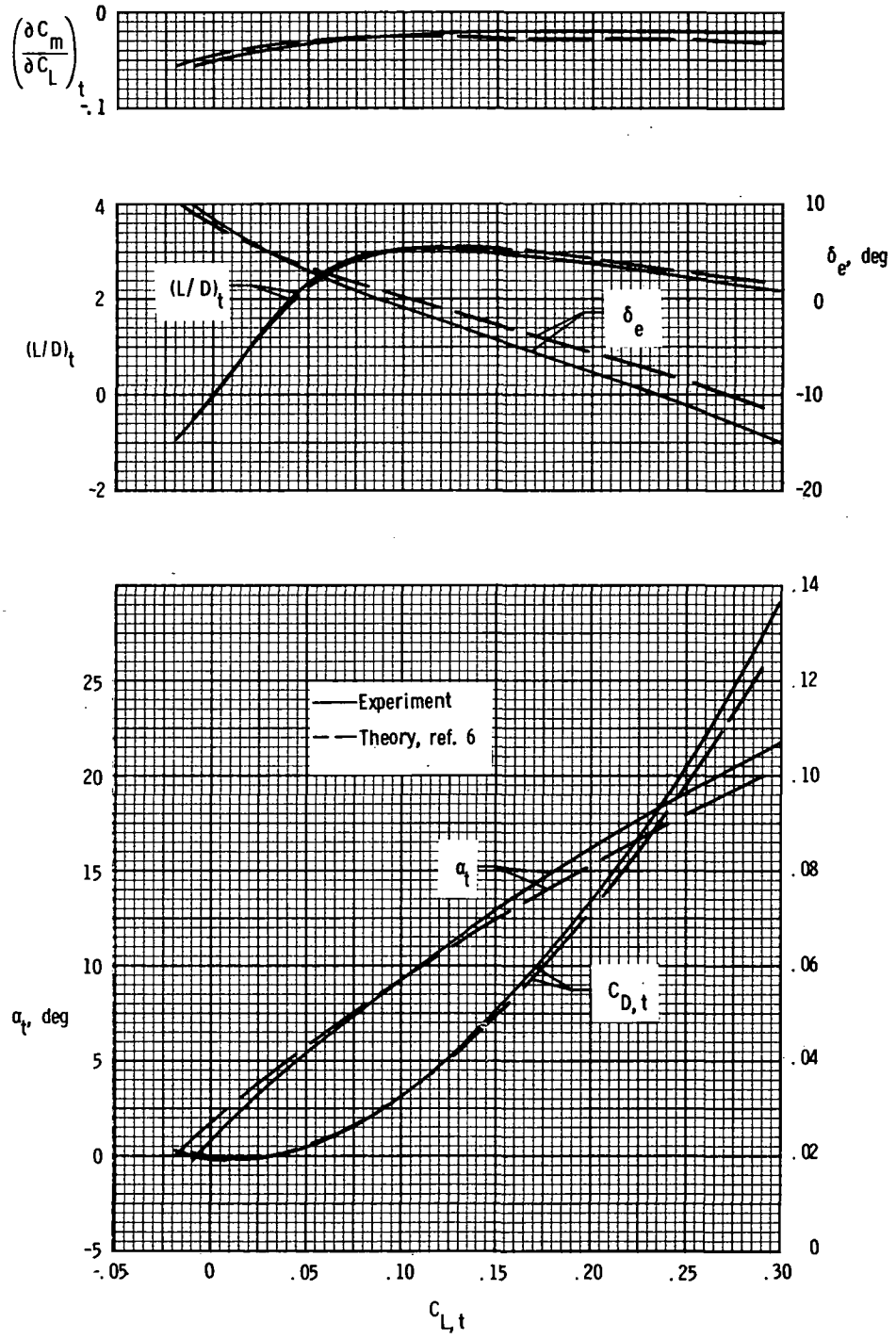


Figure 14.- Comparison of experimental and theoretical trimmed longitudinal aerodynamic characteristics of $BWV_{CH}$ configuration.

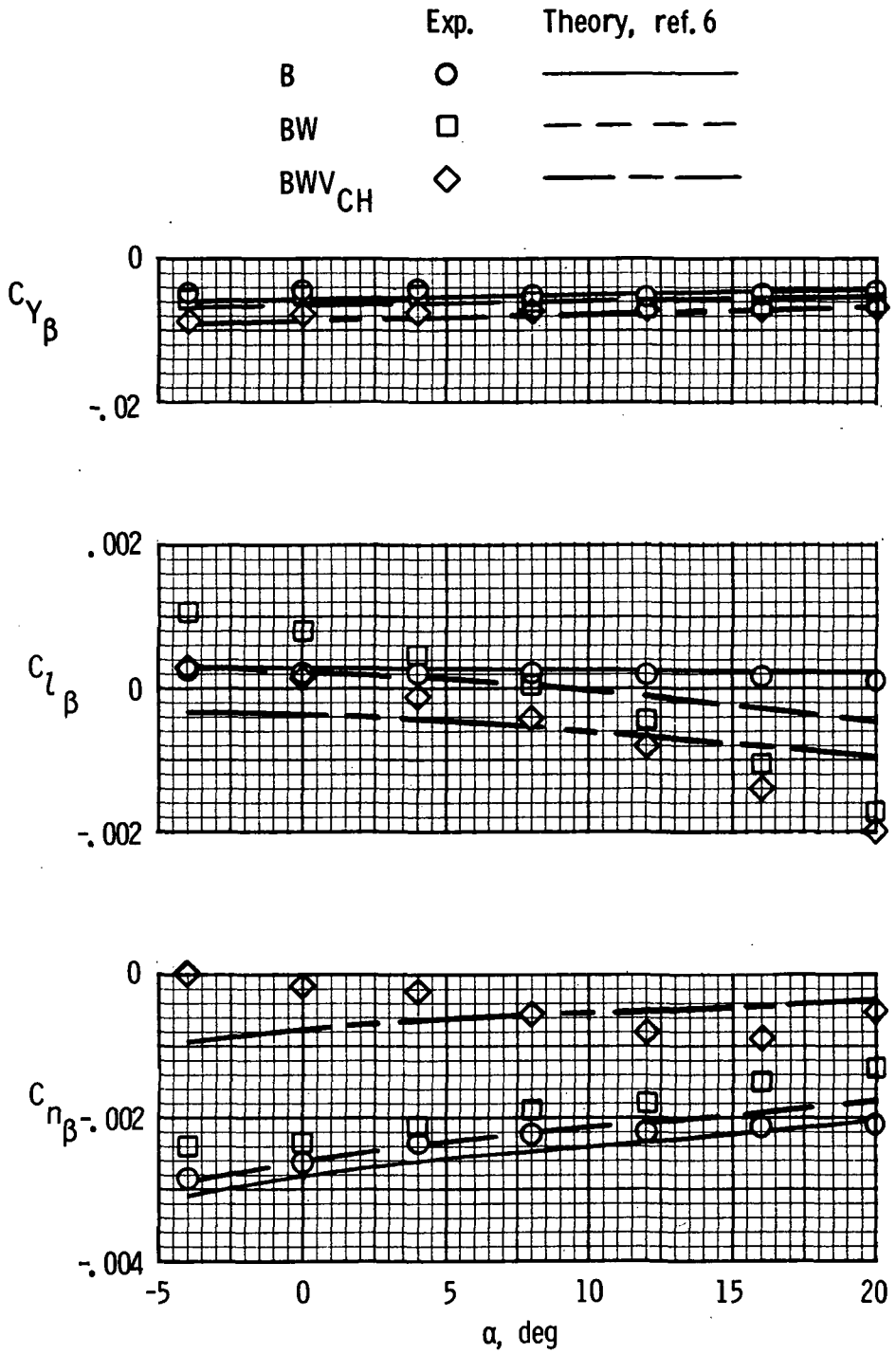


Figure 15.- Comparison of experiment with theory for effect of body buildup on static lateral-directional stability characteristics. $\Delta\beta = -2^{o}$.

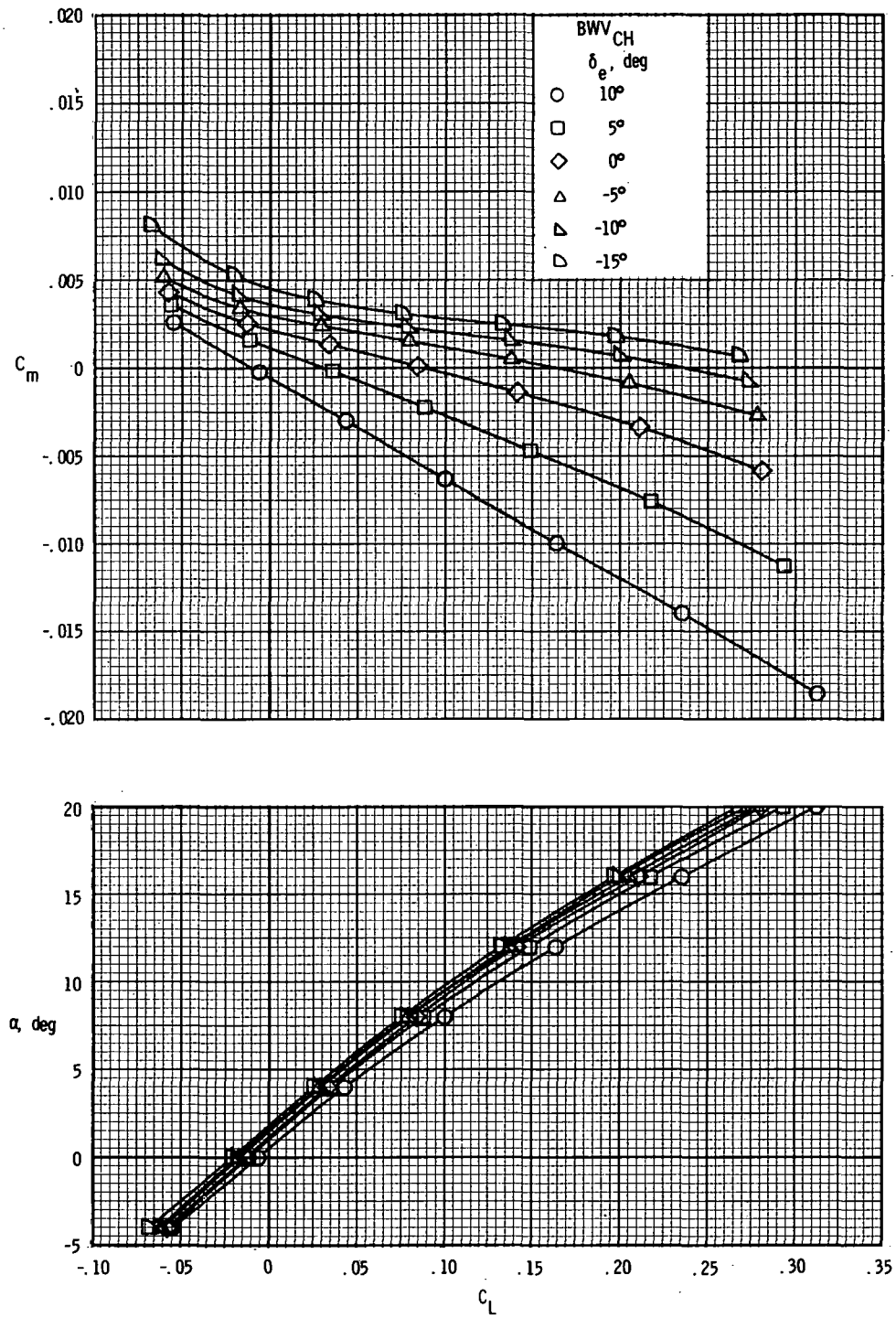


Figure 16.- Effect of elevon deflection on longitudinal aerodynamic characteristics of $BWV_{CH}$ configuration.

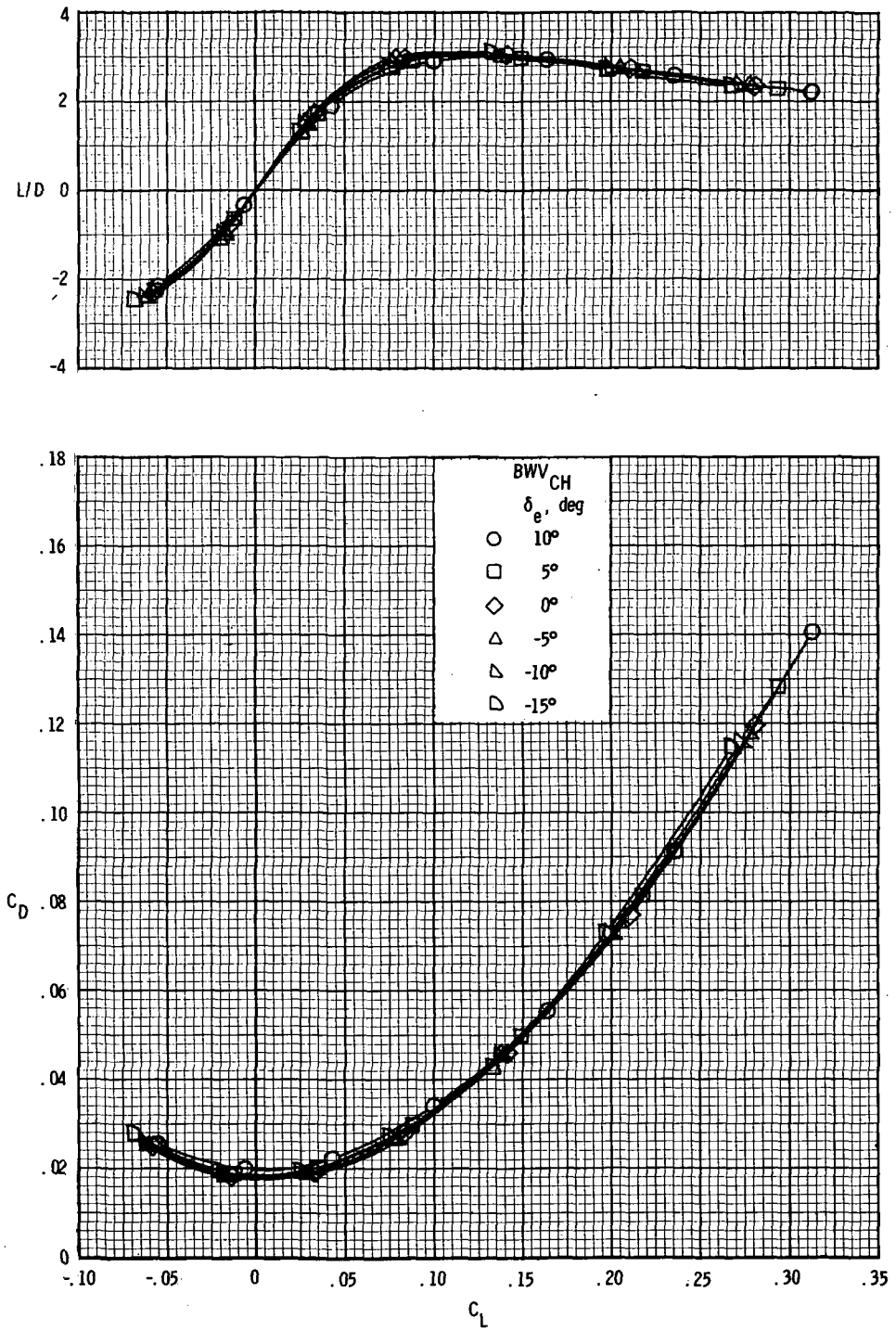


Figure 16.- Concluded.

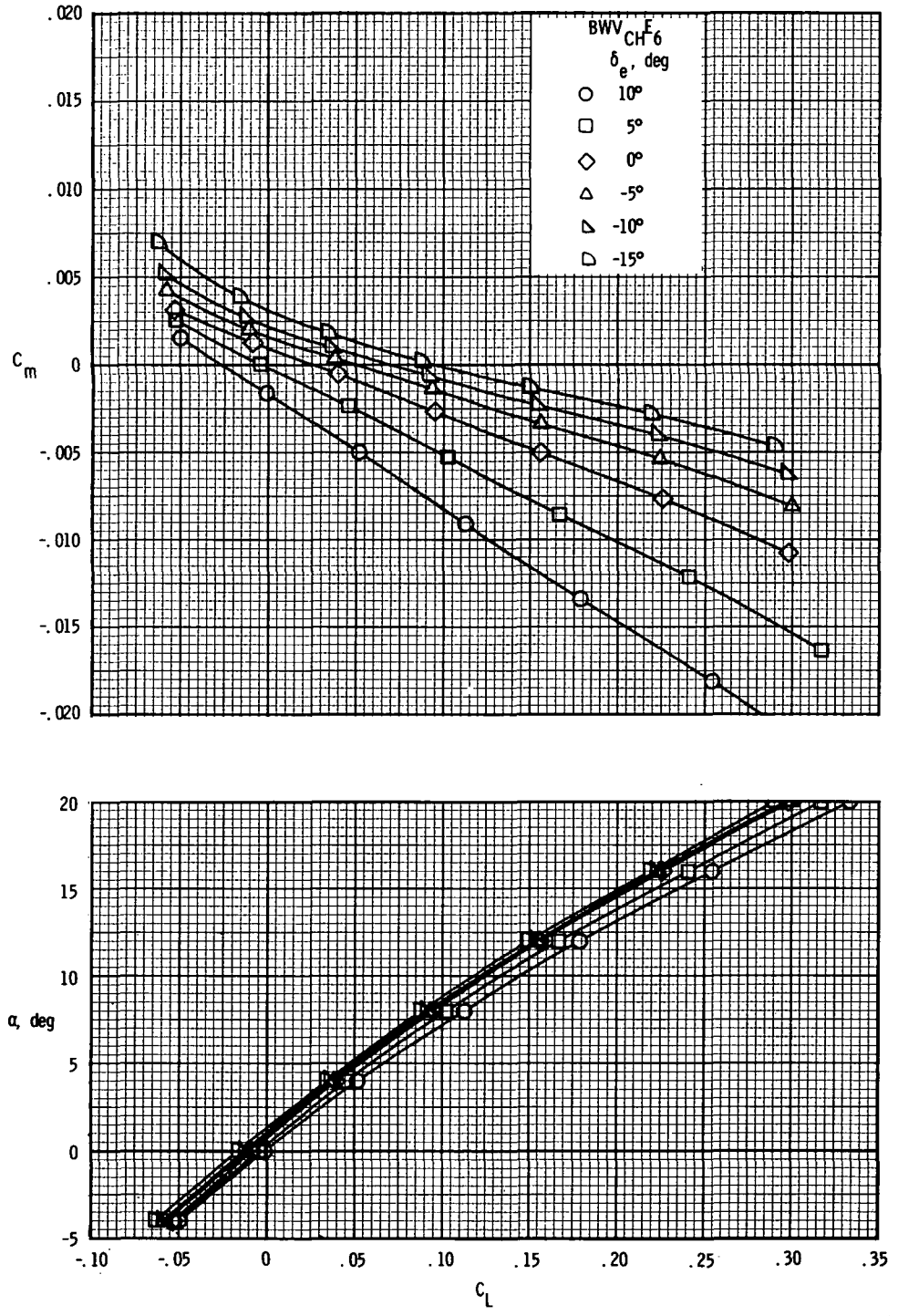


Figure 17.- Effect of elevon deflection on longitudinal aerodynamic characteristics of $BWV_{CH}E_6$ configuration.

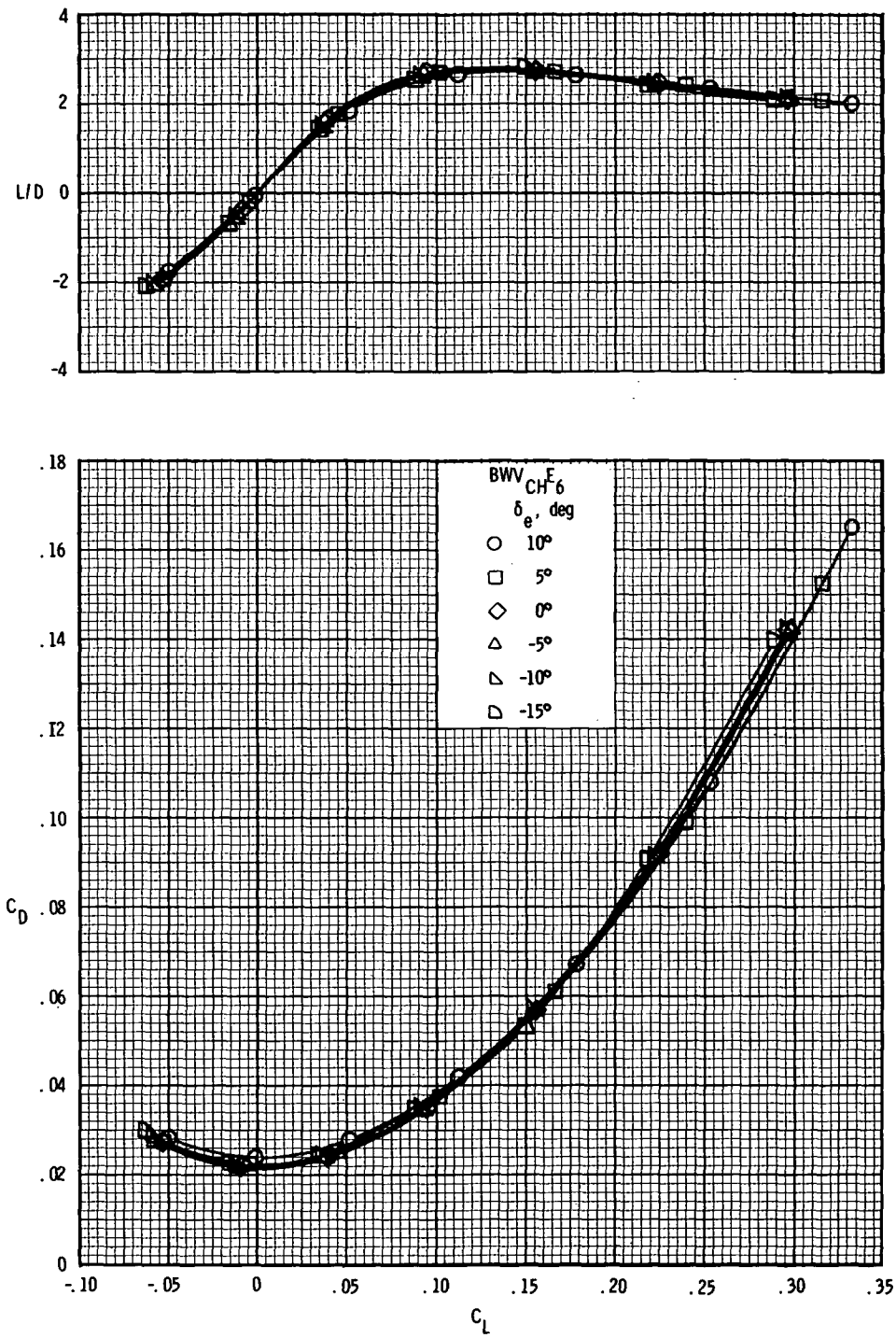


Figure 17.- Concluded.

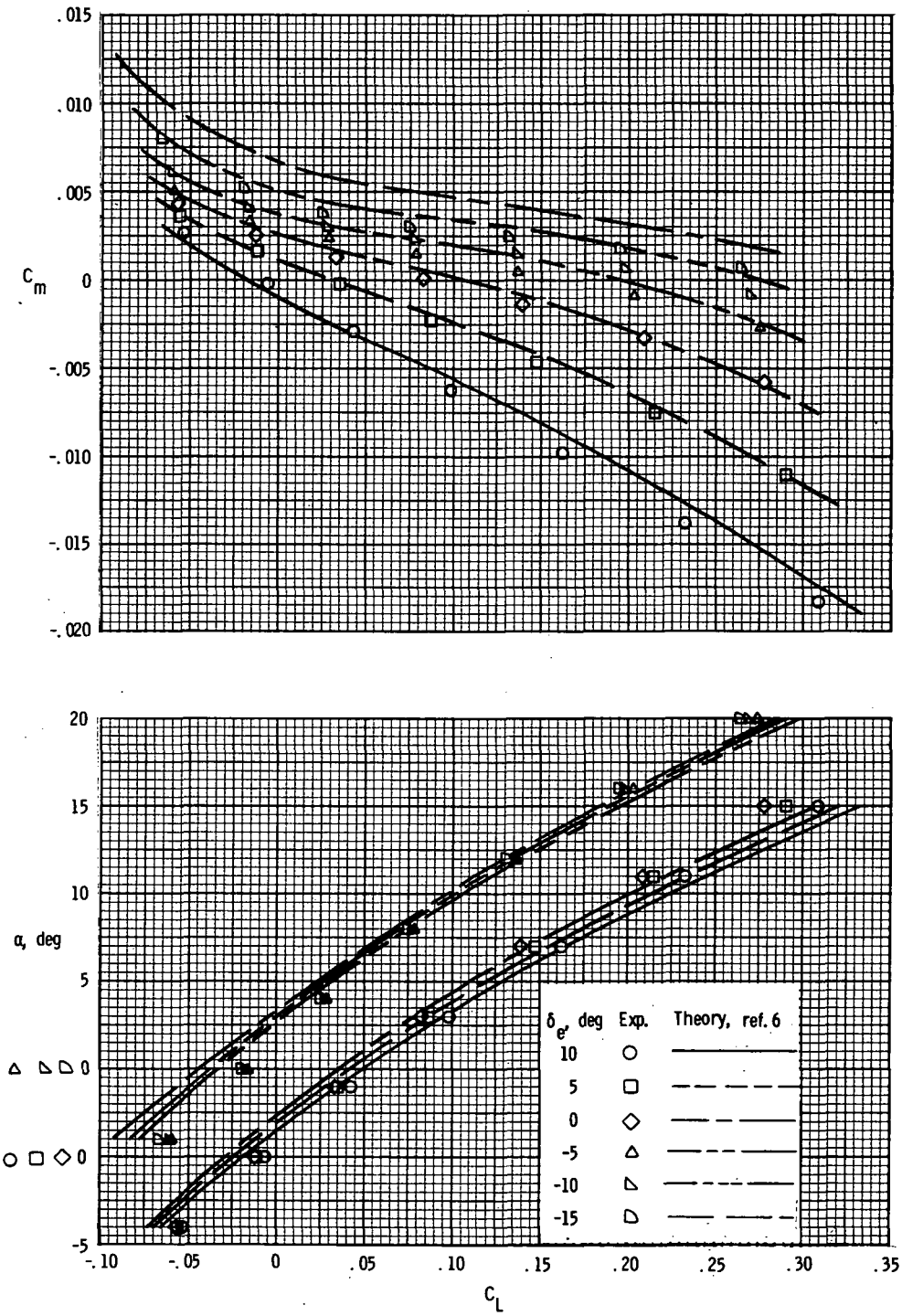


Figure 18.- Comparison of experiment with theory for effects of elevon deflection on $BWV_{CH}$ configuration.

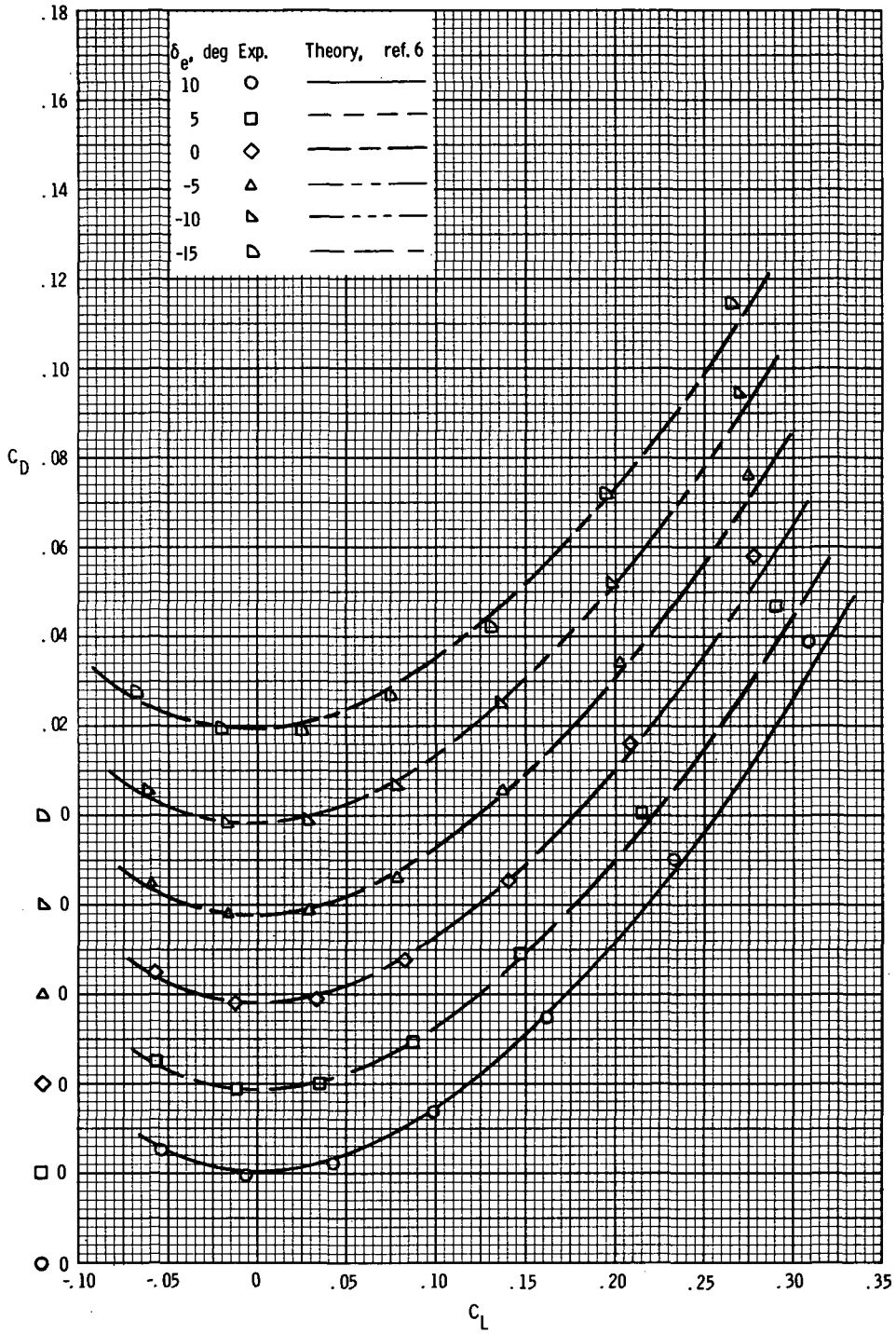


Figure 18.- Continued.

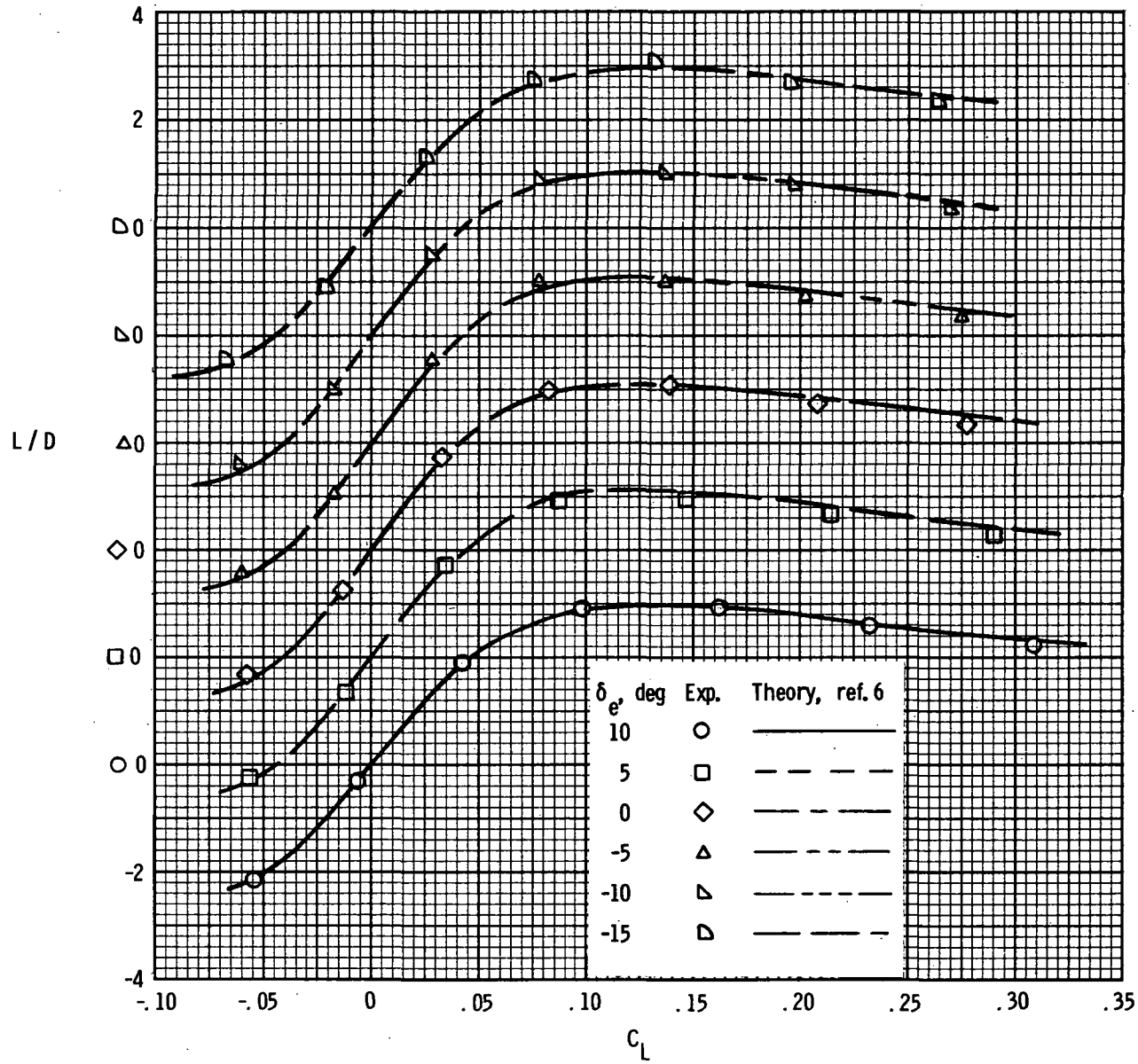


Figure 18.- Concluded.

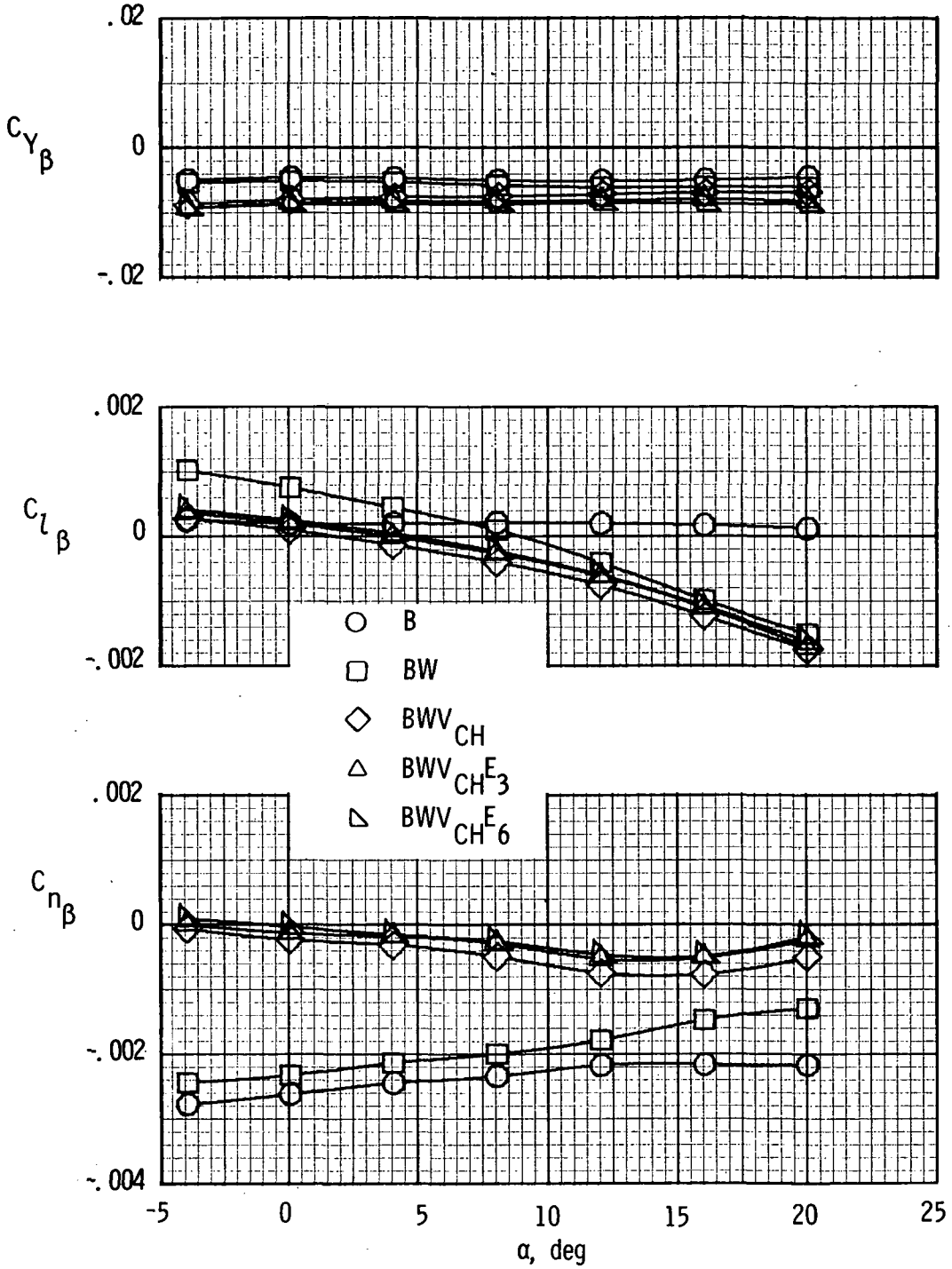


Figure 19.- Effect of body buildup on static lateral-directional stability characteristics. $\Delta\beta = -4^o$.

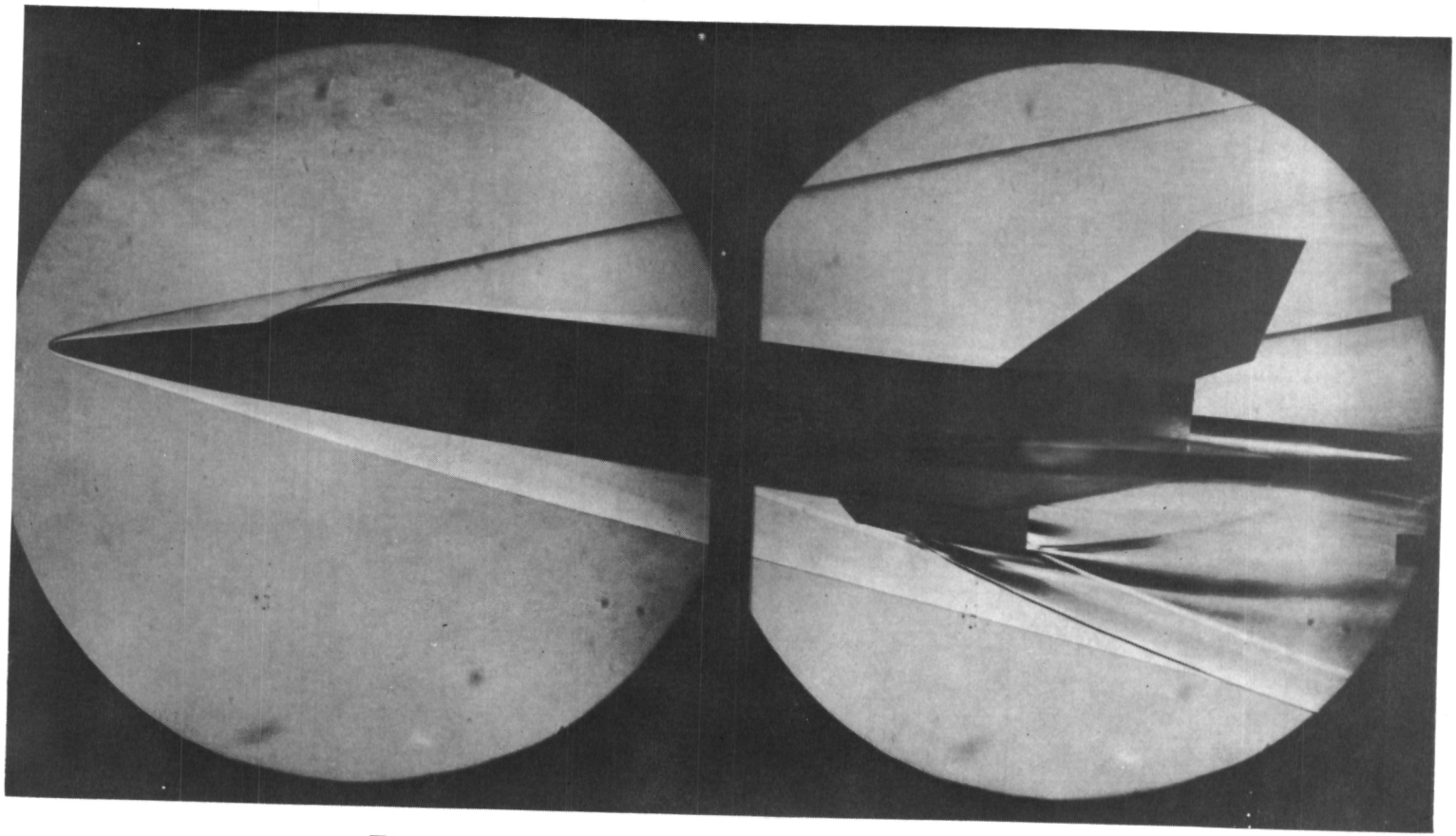

Figure 20.- Schlieren photograph of model. $\alpha = 20^{\circ}$. L-76-3470

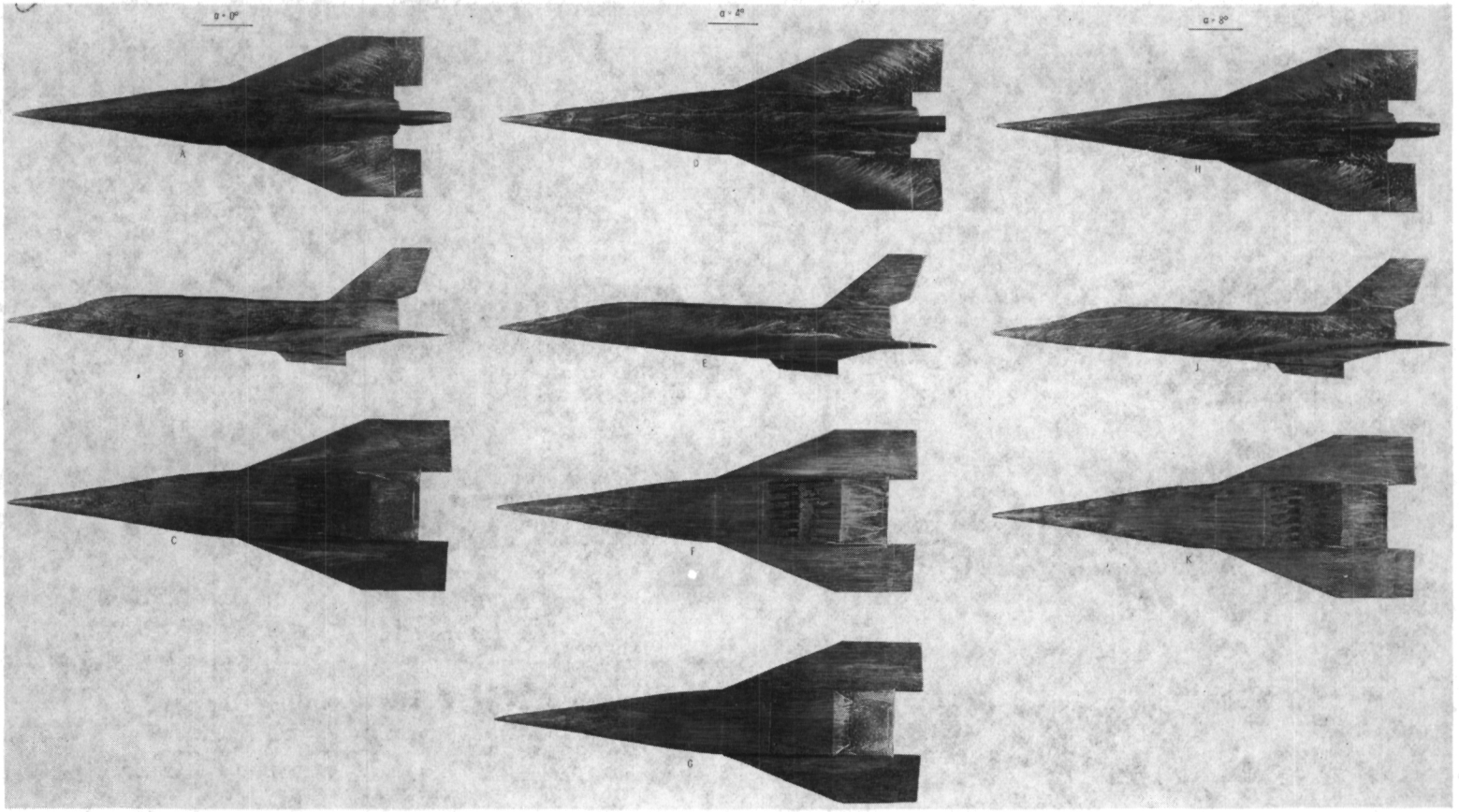

L-77-8694

(a) $\alpha = 0^{o}$, $4^{o}$, and $8^{o}$; $\beta = 0^{o}$.

Figure 21.- Oil-flow patterns on model.

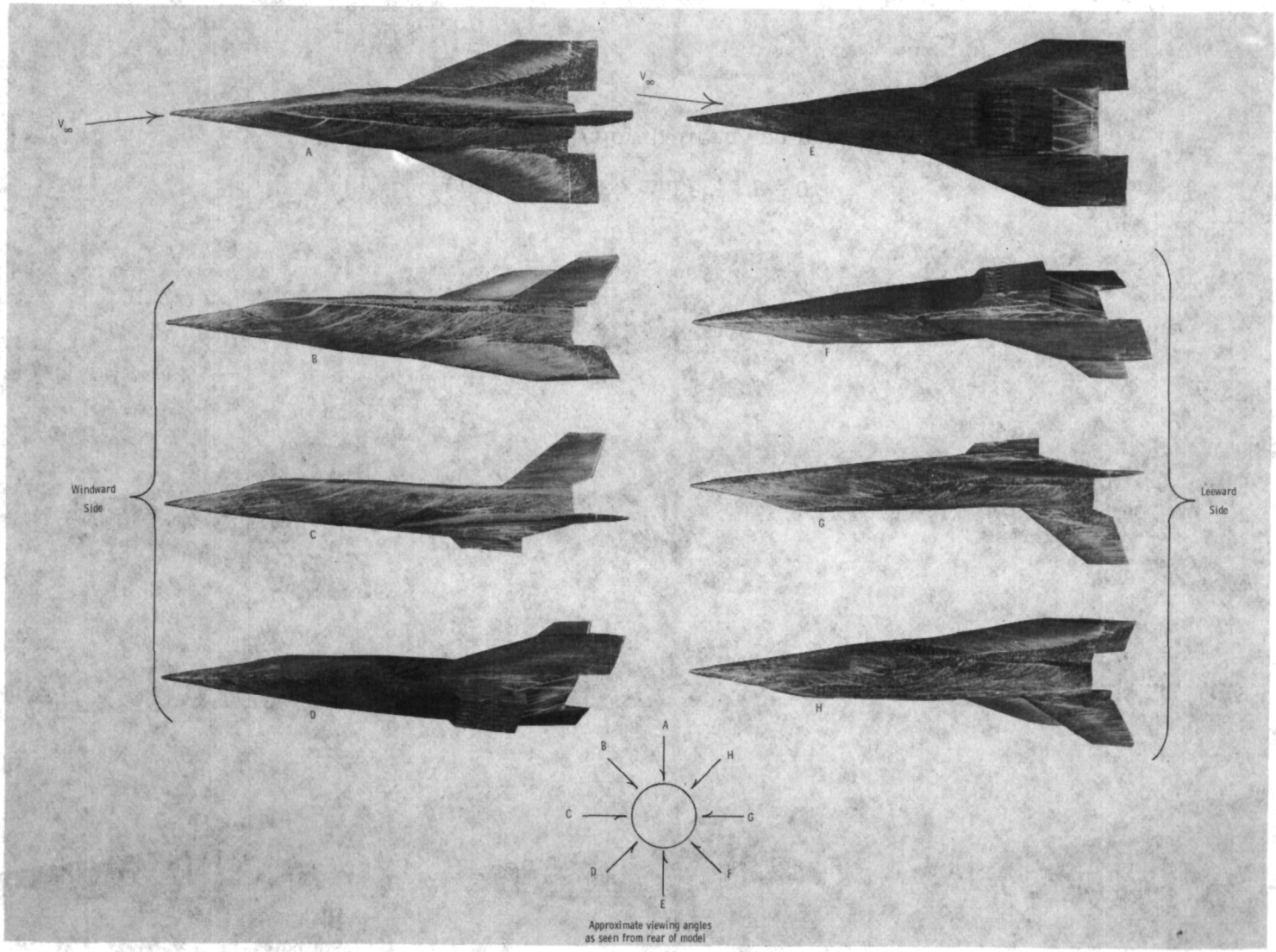


L-77-8695

(b) $\alpha = 4^o$; $\beta = -4^o$.

**Figure 21.- Concluded.**

| 1. Report No. NASA TP-1249 | 2. Government Accession No. | 3. Recipient's Catalog No. |
|---|---|---|
| 4. Title and Subtitle<br>AERODYNAMIC CHARACTERISTICS AT MACH 6 OF A WING-BODY CONCEPT FOR A HYPERSONIC RESEARCH AIRPLANE | | 5. Report Date<br>August 1978<br>6. Performing Organization Code |
| 7. Author(s)<br>James L. Dillon and Jimmy L. Pittman | | 8. Performing Organization Report No.<br>L-12183<br>10. Work Unit No.<br>505-11-33-01 |
| 9. Performing Organization Name and Address<br>NASA Langley Research Center<br>Hampton, VA 23665 | | 11. Contract or Grant No.<br>13. Type of Report and Period Covered<br>Technical Paper |
| 12. Sponsoring Agency Name and Address<br>National Aeronautics and Space Administration<br>Washington, DC 20546 | | 14. Sponsoring Agency Code |
| 15. Supplementary Notes | | |

16. Abstract

An experimental investigation of the static aerodynamic characteristics of a 1/30-scale model of a wing-body concept for a high-speed research airplane was conducted in the Langley 20-inch Mach 6 tunnel. The investigation consisted of configuration buildup from the basic body by adding a wing, center vertical tail, three-module scramjet, and six-module scramjet engine. The test Mach number was 6 at a Reynolds number, based on model fuselage length, of about $13.7 \times 10^6$. The test angle-of-attack range was $-4^\circ$ to $20^\circ$ at constant angles of sideslip of $0^\circ$, $-2^\circ$, and $-4^\circ$. The elevons were deflected from $10^\circ$ to $-15^\circ$ for pitch control. Roll and yaw control were investigated. Experimental aerodynamic characteristics are compared with analytical estimates.

| 17. Key Words (Suggested by Author(s)) | 18. Distribution Statement |
|---|---|
| Hypersonic research airplane<br>Hypersonic stability and control<br>Aerodynamic characteristics | Unclassified – Unlimited<br>Subject Category 02 |

| 19. Security Classif. (of this report) | 20. Security Classif. (of this page) | 21. No. of Pages | 22. Price* |
|---|---|---|---|
| Unclassified | Unclassified | 56 | $5.25 |

*For sale by the National Technical Information Service, Springfield, Virginia 22161

NASA-Langley, 1978

National Aeronautics and
Space Administration

Washington, D.C.
20546

Official Business
Penalty for Private Use, $300

THIRD-CLASS BULK RATE

Postage and Fees Paid
National Aeronautics and
Space Administration
NASA-451


NASA

POSTMASTER: If Undeliverable (Section 158 Postal Manual) Do Not Return